NASA CR-66743

CORRELATION OF ELECTRICAL CONDUCTIVITY AND RADIATION-INDUCED FREE RADICAL CONCENTRATION IN POLY(ETHYLENE TEREPHTHALATE) AND RELATED COMPOUNDS

By L. K. Monteith, D. T. Turner,
and L. F. Ballard

Prepared under Contract No. NAS1-7553 by
RESEARCH TRIANGLE INSTITUTE
Research Triangle Park, N. C.

for

NATIONAL AERONAUTICS AND SPACE ADMINISTRATION

ABSTRACT

This report describes a research effort concerning the electronic processes in irradiated poly(ethylene terephthalate), PET, and two model compounds. The radical concentration in PET is shown to build up continuously as the γ-dose or UV light exposure is increased. Three different radicals are identified by ESR spectra.

The relative concentration of each radical depends upon the degree of crystallinity of the sample. The optical absorption near 3100 Å and the electrical conductivity of irradiated samples are tied directly to the radical concentration. This is demonstrated by observing the rate of buildup of each effect and the kinetics of radical decay and conductivity decay at various temperatures. The quenching effect of oxygen is also shown to be similar for radical concentration, optical absorption, and electrical conductivity.

Carrier mobilities are measured for PET and molecular crystals of dimethyl terephthalate and dibenzoate ester of ethylene glycol. The mobility of the molecular crystals is observed to decrease significantly after exposure to γ-rays. Bulk and surface polarization effects are observed to play a dominant role in transient electronic behavior.

CONTENTS

LIST OF FIGURES

LIST OF FIGURES (Continued)

LIST OF FIGURES (Continued)

LIST OF TABLES

ELECTRONIC PROCESSES IN IRRADIATED ORGANIC SOLIDS

By L. K. Monteith,* D. T. Turner,** and L. F. Ballard

SECTION I

INTRODUCTION

The unique properties of organic polymers and other dielectric materials have found many uses in the environment of outer space. However, the effects of radiation on these materials have been difficult to analyze in the key area of chemical and physical changes which affect electronic properties. Toward this end we have directed a research effort to determine the effects of gamma and ultra-violet radiation on the electronic properties of poly(ethylene terephthalate), PET, and its related model compounds. Particular emphasis has been upon the formation of free radicals and their relation to the electrical conductivity. As a related effort, the charge storage and breakdown characteristics of some silicon oxides in a radiation environment were studied.

---

* Now at North Carolina State University, Raleigh, N. C.

** Now at Drexel Institute, Philadelphia, Pennsylvania.

SECTION II

RADIATION INDUCED RADICAL FORMATION IN PET

2.1 Absorption of Light by Free Radicals

Preliminary experiments with PET led to the belief that free radicals were absorbing light. A search of the literature revealed a report that free radicals formed in polyethylene by exposure to high energy radiation do absorb light strongly [Ref. 1a]. This observation raises the general question of how the properties of a polymer exposed to high energy or ultra-violet radiation in a space environment might be modified due to accumulation of trapped radicals. The question was pursued with respect to changes of light absorption due to radicals introduced by exposure of PET films to either γ-rays or to ultra-violet light and with respect to the influence of the radical concentration on photoconductivity.

Changes in absorption following γ-irradiation. - Samples of PET ($3 \times 1 \times 0.0025$ cm^3) were thoroughly degassed and sealed in vacuum or in nitrogen in Pyrex ampuls. These samples were exposed to Co-60 γ-rays at a dose rate of 0.5 Megarad/hr (Mrad/hr), at about 35°C, along with similar samples which were irradiated in air. After an energy deposition of 189 Mrad the samples were removed from the ampuls and, in a matter of minutes, the absorption spectra recorded in air using a Perkin-Elmer Spectrophotometer (Model 202). Further spectra were recorded periodically until no further changes in spectra could be detected. The post-irradiation changes in absorbance ($\log_{10} \frac{I_o}{I}$) obtained for a sample which had been irradiated in vacuum are shown in Fig. 1. Closely similar results were obtained with samples irradiated in nitrogen but these are not shown. By contrast, no post-irradiation changes were detected for samples irradiated in air (Fig. 2).

Changes in absorption following u-v irradiation. - A sample of PET ($3 \times 1 \times 0.0025$ cm^3) was placed in a rectangular quartz cell with optically clear windows and the absorption spectrum recorded (Fig. 3). The spectrum changed only slightly as a result of thoroughly degassing the sample and sealing in vacuum. Exposure to a medium pressure mercury arc (Hanovia 654 A10) through 1 mm Pyrex for 16 hours with an incident energy on the film of the order 10^{-5} Einsteins/cm^2/hr resulted in an increased absorbance (Fig. 3). As in the case of γ-irradiated samples, the absorbance subsequently decreased when the irradiated sample was exposed to air. Results obtained after contact with air for 3 hours followed by degassing and sealing in vacuum are as shown in Fig. 3.

Preliminary attempts to get better resolved difference spectra with

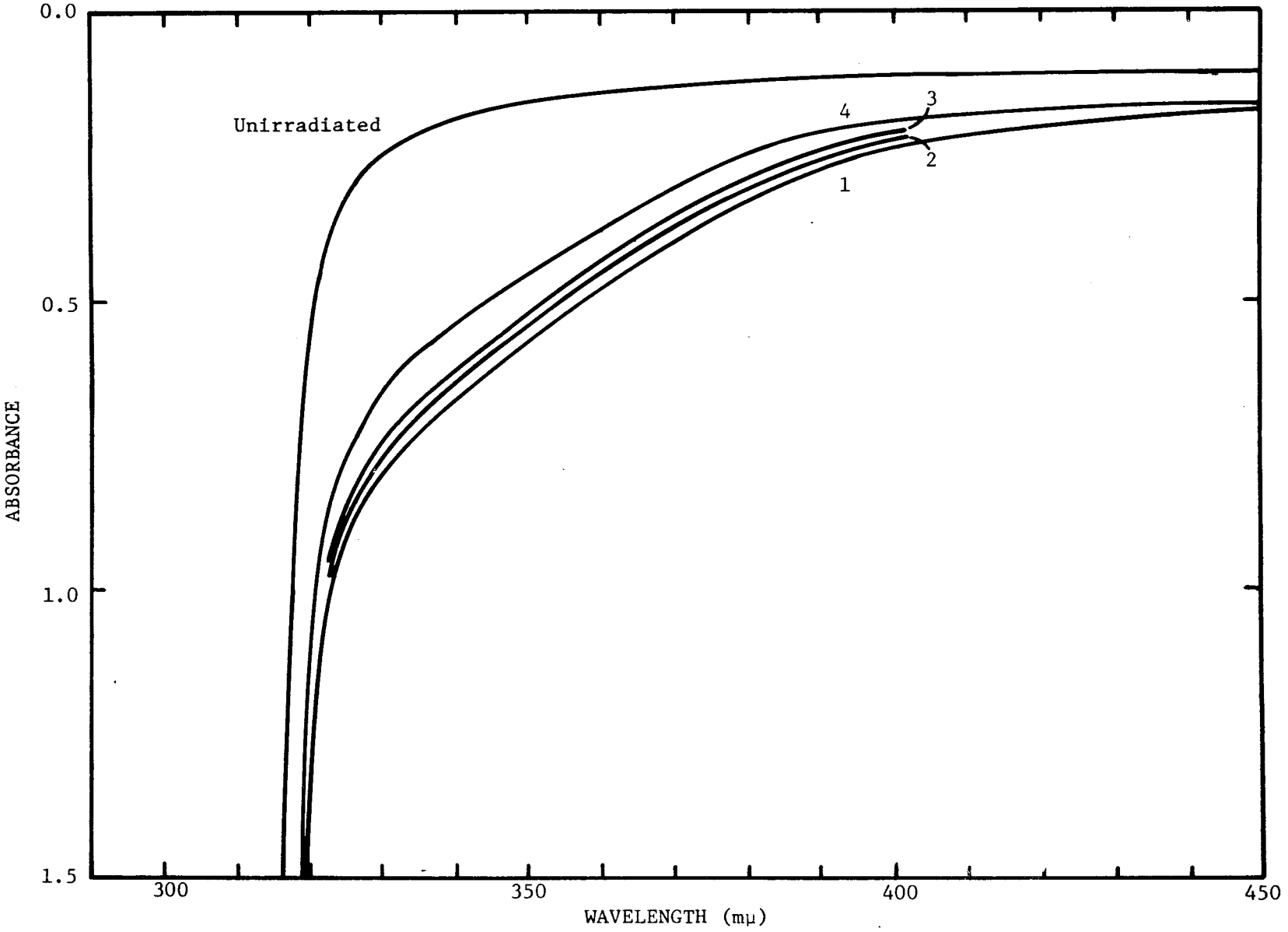

Figure 1. ABSORBANCE OF PET EXPOSED TO γ-RAYS IN VACUUM AND AFTER CONTACT WITH AIR. Dose: 189 Mrad. Time after exposure to air: 1. 15 mins, 2. 30 mins, 3. 240 mins, and 4. 3840 mins.

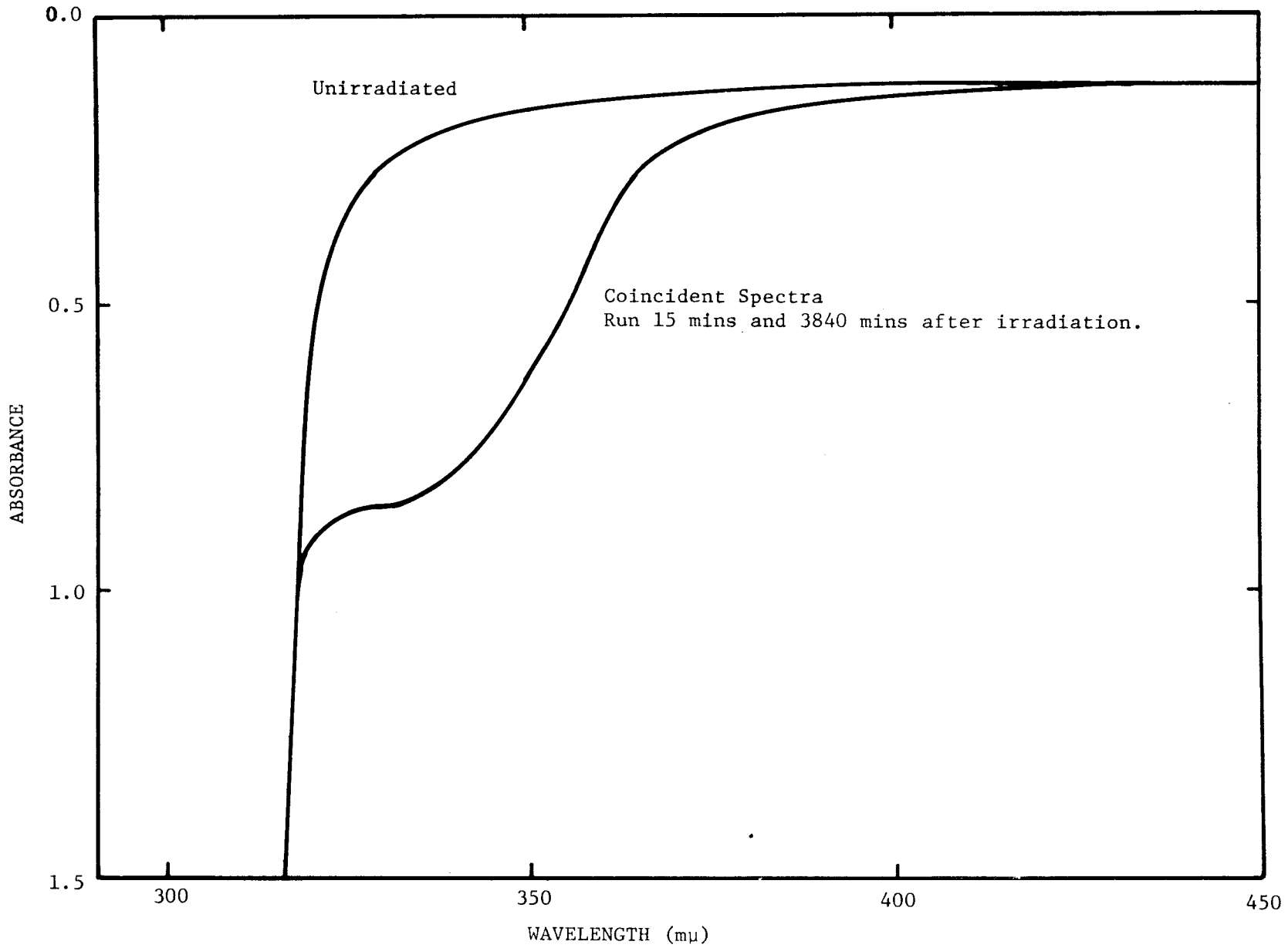

Figure 2. ABSORBANCE OF PET EXPOSED TO γ-RAYS IN AIR AND AFTER CONACT WITH AIR.
Dose: 189 Mrad

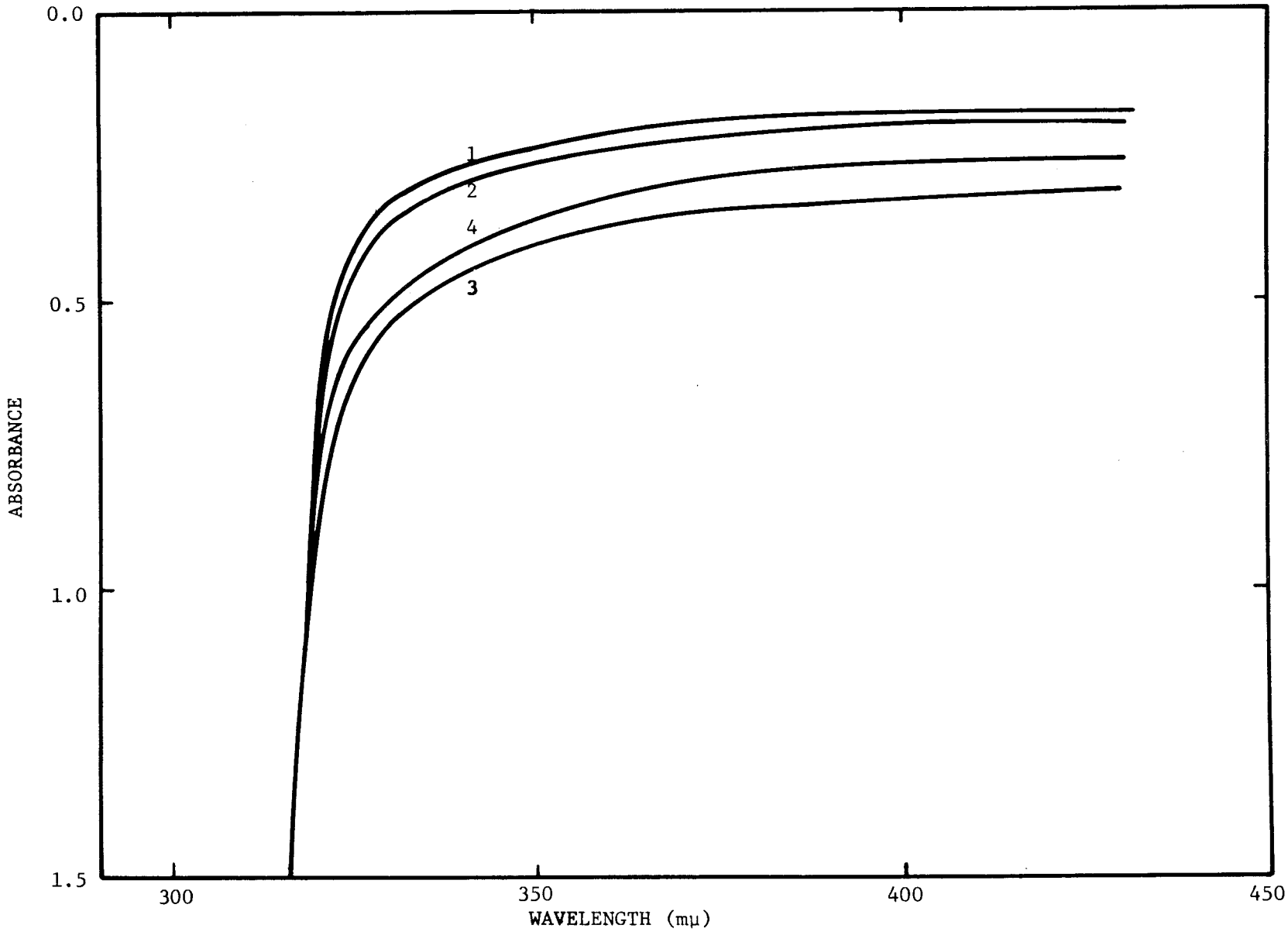

Figure 3. ABSORBANCE OF PET EXPOSED TO ULTRAVIOLET LIGHT IN VACUUM AND AFTER CONTACT WITH AIR. 1. Unirradiated in air, 2. Unirradiated in vacuum, 3. 3 hours after opening, and 4. 3 hours after opening 3 to air followed by re-evacuation.

thin films (500 Å) cast from trifluoroacetic acid were encouraging but the specially designed quartz cell was broken before definitive results could be obtained.

Discussion. - Irradiation of PET, either with γ-rays or ultra-violet light, in the absence of air results in a general increase in absorbance at wavelengths > 3100 Å (Figs. 1 to 3). In the cases where oxygen was excluded during irradiation the absorbance decreased on subsequent post-irradiation access of air. It is known that irradiation results in radical trapping and that the radicals are destroyed by access to oxygen. Therefore, the obvious explanation of these observations is that the radicals have a high extinction coefficient. An order of magnitude estimate from the data in Fig. 1 (along with ESR data giving ca 10^{18} radicals/g) gives a value for the molar extinction coefficient of 3500 $mole^{-1} liter\ cm^{-1}$ (3300-3800 Å); this is similar to the value reported for trapped radicals in polyethylene. More precise estimates at better defined wavelengths might be obtained using more transparent thin films but as mentioned previously this was attempted but not realized experimentally.

The observation that trapped radicals absorb a significant amount of light is of interest in two respects. First, it could seem to provide a reasonable explanation of post-irradiation changes in absorbance which were on record in the literature in connection with the possible use of PET as a dosimeter suitable for high doses of radiation. Second, it suggests that attention be given to the possibility that the properties of PET might change with time due to accumulation of radicals. Within the framework of the present contract this possibility was explored in relation to measurements of photoconductivity.

2.2 Post Irradiation Free Radical Reactions

The rate at which free radicals disappear during the post irradiation heating of a polymer depends on their distribution and movement. Eventually, after disappearance of closely spaced radicals, the remaining population may be sufficiently random for the subsequent decay to conform to simple second-order kinetics. This poses an interesting question about the process which permits polymer radicals to come together over an average distance as great as 100 Å as would be necessary for decay in a sample containing 10^{18} radicals/cm^3. In the case of an amorphous sample of polymethylmethacrylate (T_g=104°C), Ohnishi and Nitta pointed to the correspondence of their experimental value of 28 Kcal/mole to the activation energy of the second order radical decay with a value of 27 ±10 Kcal/mole obtained from NMR measurements. They concluded that both processes were due to motions of segments of the polymer molecules [Ref. 1b]. Notwithstanding, it seemed surprising that the decay occurred in the temperature range of 28 to 55°C which is considerably below the glass transition temperature of about 70°C for PET.

This type of difficulty seems so extreme in the case of similar studies of a partially crystalline sample of nylon-6 that Ballentine and Shinohara invoked the idea that radical sites can move along and between polymer chains by a sequence of hydrogen atom shifts, i.e., by repetition of chemical reactions of the kind $RH + R'\cdot \rightarrow R\cdot + R'H$ [Ref. 2]. Earlier this idea of radical site migration had been introduced by Dole, Keeling, and Rose to account for certain features of the irradiation chemistry of polyethylene [Ref. 3] and recently a good case has been made by Gehmer and Wagner [Ref. 4] that such a process could account quantitatively for the magnitude of the second order rate constant reported by Charlesby, Libby, and Ormerod for the post-radiation decay of alkyl radicals in polyethylene [Ref. 5]. On the other hand, Auerbach has presented detailed evidence that the rate of decay of alkyl radicals in polyethylene correlates closely with the temperature range in which the polymer is known to change from a glassy to a viscoelastic material and concluded that the process is controlled by normal diffusion [Ref. 6]. A puzzling feature of this latter picture is that it seems to account for the whole radical population by reference to the amorphous content which composes only about 20% of the polymer.

At present, it does not seem to be possible to decide between physical and chemical processes of radical movement in polymers. One long range approach to the problem is to document radical decay processes further and to urge their continued consideration alongside the development of other diverse methods of assessing movement in polymers. Eventually, it should then be possible to judge more critically any cases in which physical movement appears to be inadequate. In this further documentation, it seems judicious to make a clear distinction between processes in amorphous and crystalline regions. The following are some experiments in this direction with PET.

Experimental. - The samples were biaxially oriented film of thickness 0.0025 cm (Mylar C: DuPont) of about 50% crystallinity, an amorphous precursor of thickness 0.03 cm and a polycrystalline sample of about 70% crystallinity obtained by heating the amorphous sample for 48 hours at 235-240°C in a vacuum and cooling slowly [Ref. 8]. The crystalline content was estimated from x-ray defraction data.

Samples were thoroughly degassed and sealed in Suprasil quartz tubes at a pressure less than 10^{-4} Torr. Sheetlets from the oriented film were packed in stacks of about 30 to a total weight of about 0.5 grams. (For other details see reference 9.) After irradiation with Cobalt-60 γ-rays at a dose rate of 0.3 to 0.5 Mrad per hour the quartz was annealed at alternate ends in a flame and first and second derivatives of the absorption curve recorded at room temperature with a Varian V4502-10 spectrometer. The number of free radicals in the sample was estimated by double integration of the first derivative spectrum and comparison with α - α' - diphenyl - β - picrylhydrazyl or, relatively, by reference to a peak height. The latter method was especially convenient in following the disappearance of radicals resulting from immersion of the Suprasil tubes in a silicone oil bath

maintained constant within ±0.005°C. The two methods gave closely similar estimates up to doses of about 80 Mrads but differed somewhat in peak height at higher doses (o,◑) and double integration values (◆) for the same samples in Fig. 4.

Accumulation of Radicals. - As in the case of oriented films of PET, both amorphous and polycrystalline samples gave a featureless ESR spectrum when examined at -196°C following irradiation at this temperature. Upon warming to room temperature the number of spins decreased by about 1 order of magnitude, presumably due to the loss of charged species by recombination. The residual signal from the polycrystalline samples was found to comprise superimposed sets of six and eight lines which could be assigned to different orientations of radical I. The signal from the amorphous sample was poorly resolved but obviously quite different. It has been assigned tentatively to radical II. In addition, both samples include a central singlet spectral component which has not been assigned [Ref. 9].

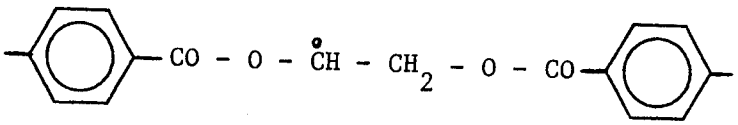

I

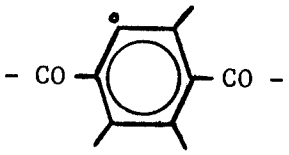

II

Despite the qualitative differences mentioned above, the total concentrations of radicals trapped in amorphous and polycrystalline samples of PET at room temperature, following irradiation at -196°C, were closely similar as may be seen by comparison of the squares and triangles to the circles in Fig. 4. When comparisons were made following irradiation at room temperature,

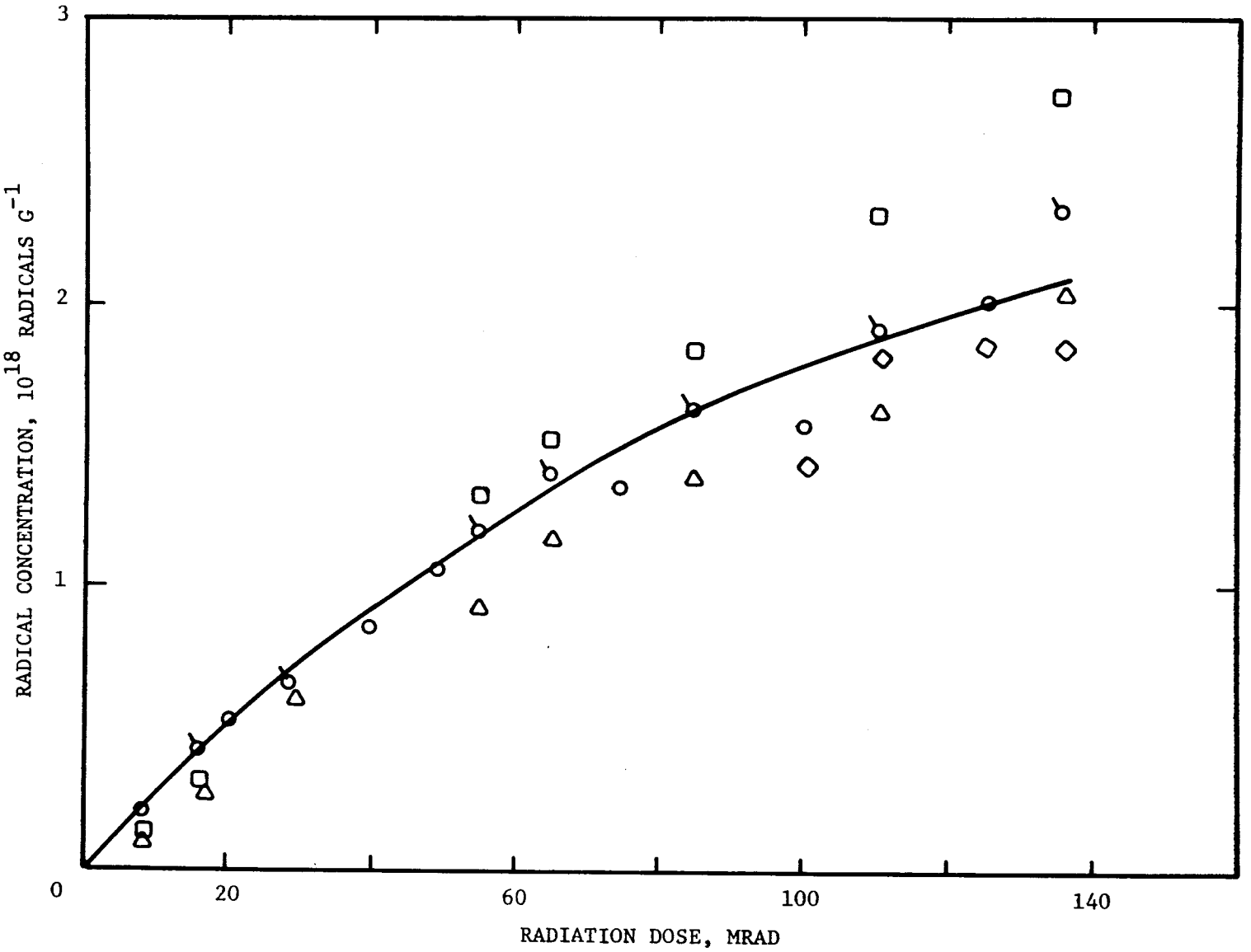

Figure 4 . ACCUMULATION OF FREE RADICALS WITH DOSE IN AMORPHOUS AND POLYCRYSTALLINE SAMPLES OF POLY(ETHYLENE TEREPHTHALATE).
□- - - 25°C, crystalline; △- - - -196°C, crystalline; ○- - - -196°C, amorphous, ♂- - - 25°C, amorphous; ◇- - - checked by double integration.

it was found that after higher doses fewer radicals had accumulated in the amorphous sample presumably because it is a less efficient trapping medium, c.f., the square symbols in Fig. 4. On the other hand, after low doses there may be slightly more radicals in the amorphous samples indicating a higher G(radical) value than in the crystalline regions. However, it should be noted that this effect would appear small when contrasted with the claim that in the case of polyethylene radicals are generated much more efficiently in glassy than in crystalline regions [Ref. 10].

Decay of Radicals in Amorphous Samples. - When a pre-irradiated amorphous sample is heated above room temperature, while still sealed in the Suprasil tube, the radicals disappear and the singlet component increases relative to the signal assigned to radical II. The overall rate of disappearance was followed by measurement of the peak height of the first derivative spectrum. The data were obtained with samples which had been given the following doses at room temperature 60°: (300 Mrad); 65°, 70°, 75°, and 77° (40 Mrad); 80°C (225 Mrad); Fig. 5. As comparisons are being made with samples given varying doses it should be pointed out that this variable was found to be unimportant in these studies. For convenience of presentation, all these results have been normalized to the same initial concentration of radicals.

Following an initially more rapid rate, the disappearance of radicals settles down to a linear relationship between the reciprocal of the concentration of radicals and time, i.e., in conformity with a second order rate reaction as required by Eq. (2.1) in which [R] and $[R_o]$ are, respectively, radical concentrations at times t and zero (Fig. 6). Values of the rate

$$\frac{1}{[R]} - \frac{1}{[R_o]} = kt \qquad (2.1)$$

constant k, obtained from the slopes in Fig. 6, have been plotted as a function of temperature according to the conventional Arrhenius equation, $k = A \exp(-E/RT)$, in Fig. 7. If the data are taken to define two lines, as shown in Fig. 7, these intersect at a point corresponding to a temperature of 72°C and give activation energies, E, of 112 and roughly, 25 Kcal/mole. As the glass transition temperature, T_g, of amorphous PET is about 70° [Ref. 11] and as large increases of activation energy for various physical processes are on record in transversing T_g, for both low and high molecular weight compounds, these findings appear reasonable [Ref. 12]. Previously, the post-irradiation decay of free radicals through T_g has been studied in the case of polymethylmethacrylate but, apparently, the results did not conform to simple kinetics and activation energies were not determined [Ref. 13].

The movement of segments of polymer molecules over distances of about

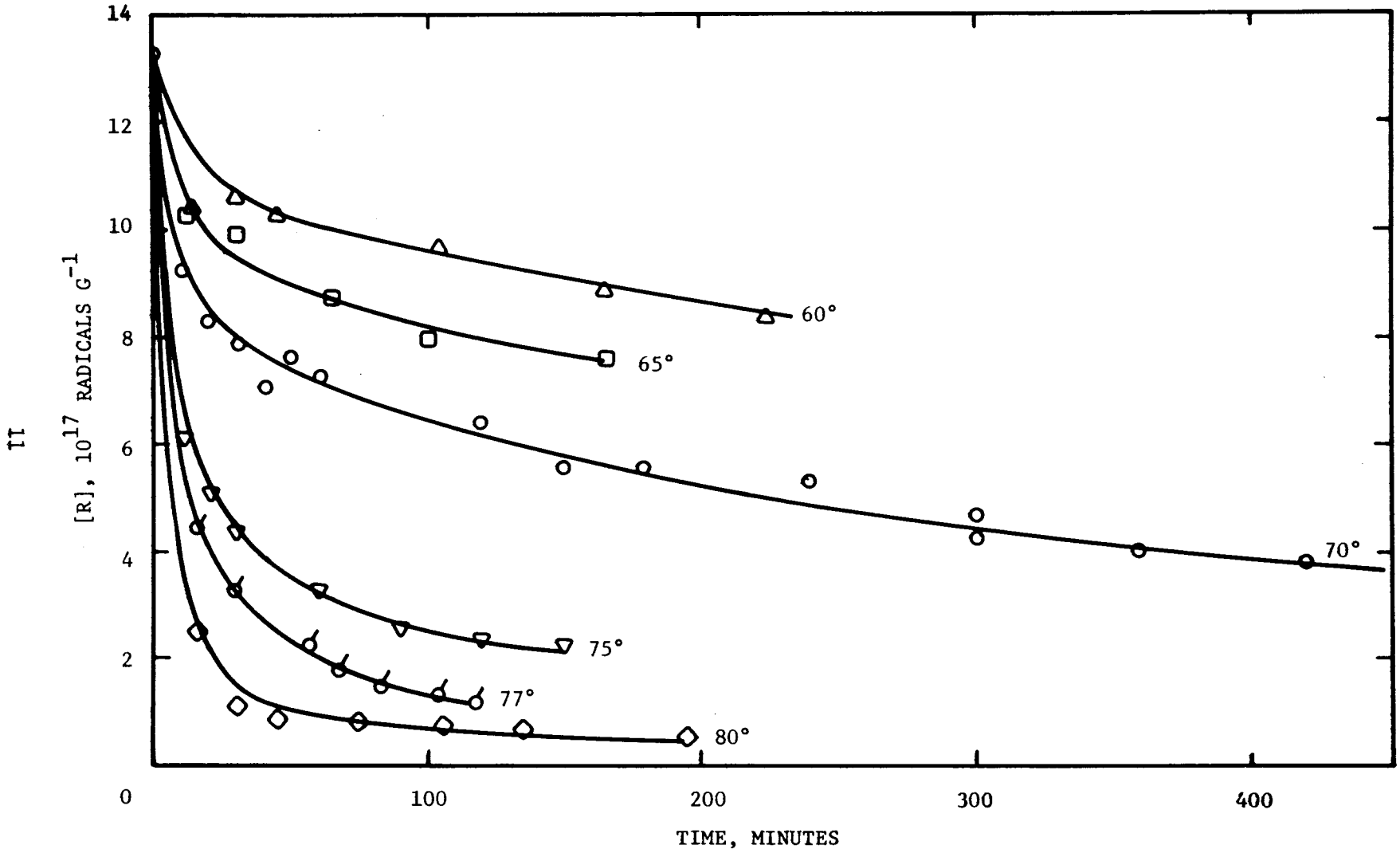

Figure 5. DECAY OF FREE RADICALS IN AMORPHOUS POLY(ETHYLENE TEREPHTHALATE)

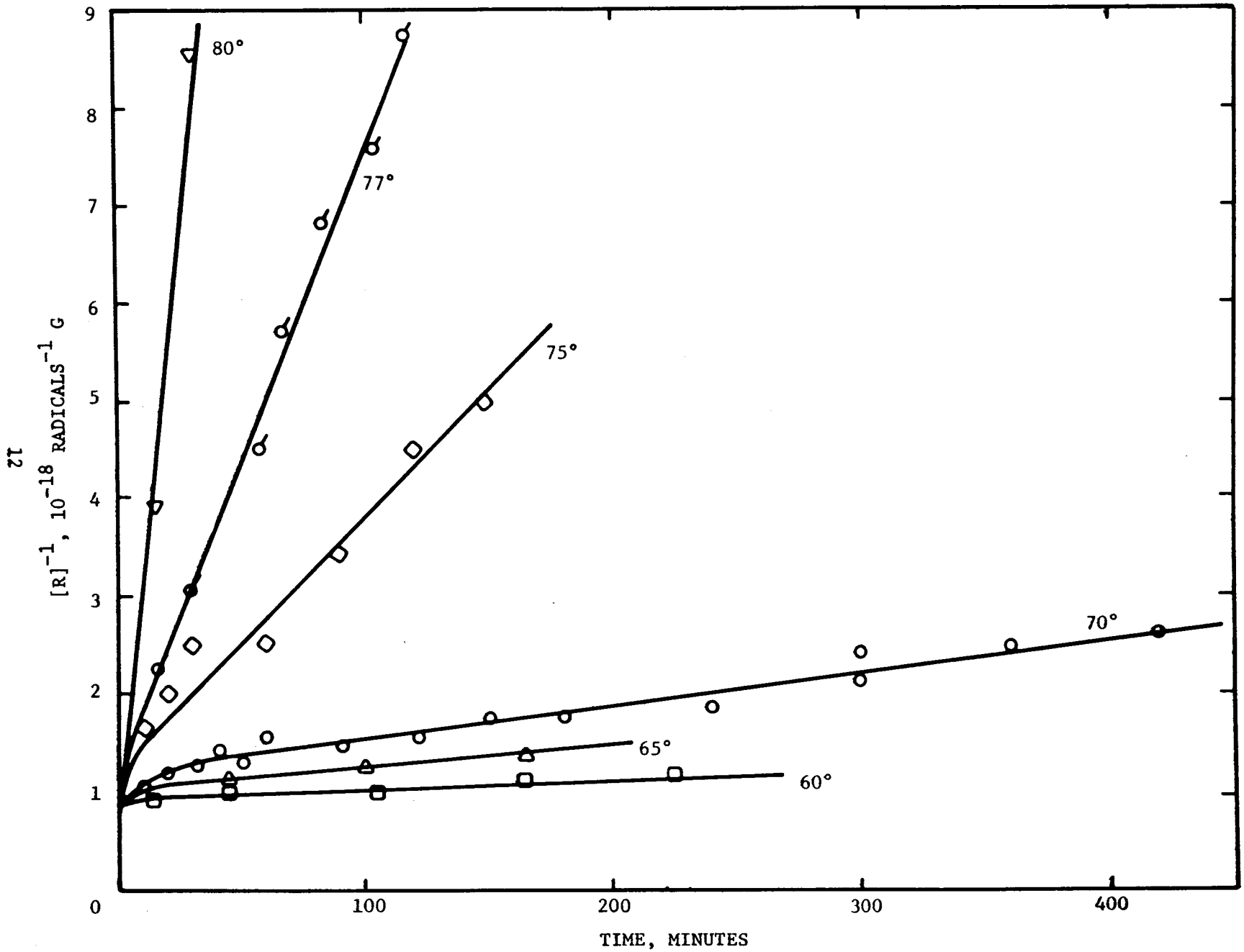

Figure 6. SECOND ORDER PLOTS FOR DECAY OF FREE RADICALS IN AMORPHOUS POLY(ETHYLENE TEREPHTHALATE).

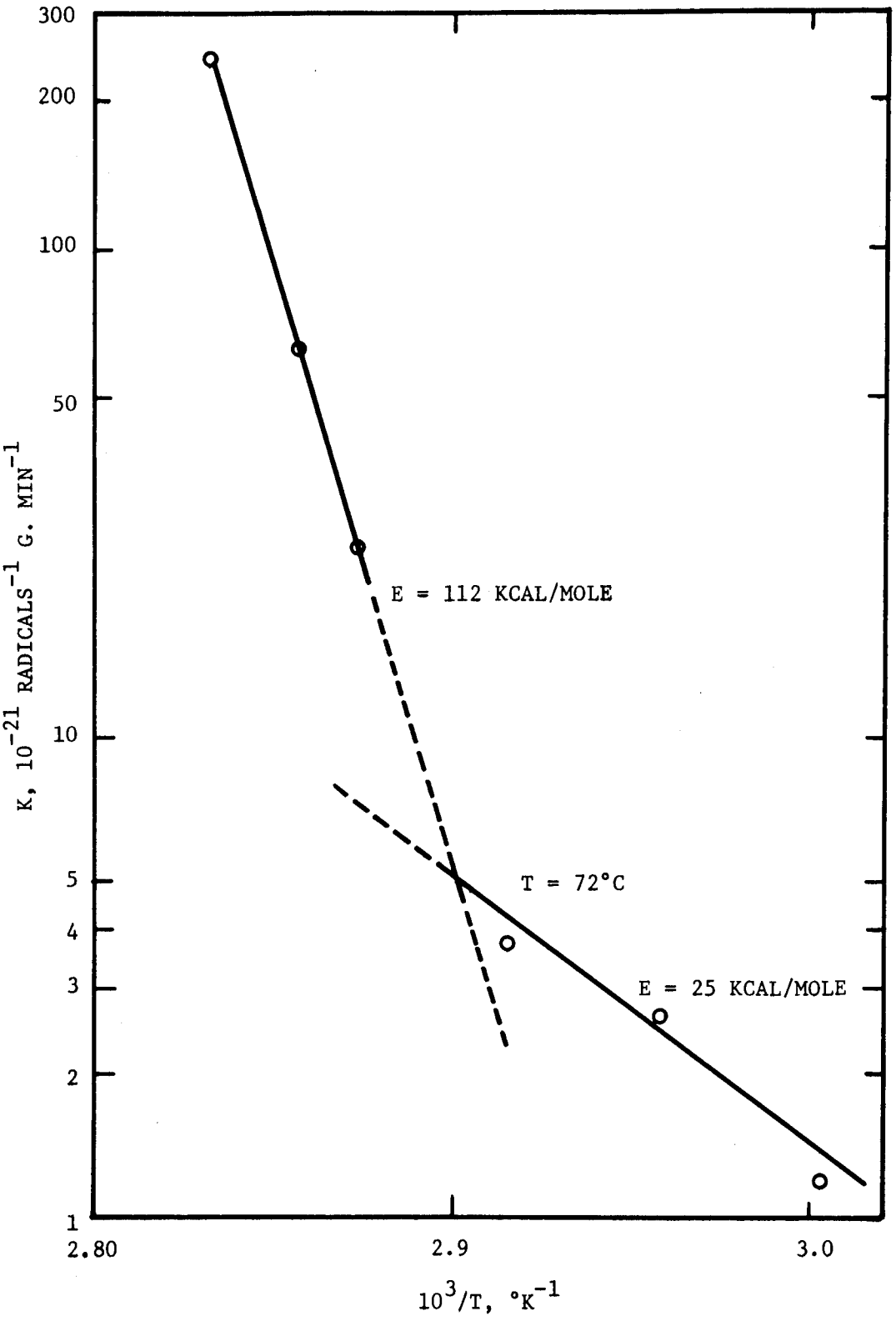

Figure 7. ARRHENIUS PLOT FOR DECAY OF RADICALS IN AMORPHOUS POLY(ETHYLENE-TEREPHTHALATE)

10^2 Å is readily acceptable as a plausible mechanism of polymer radical decay above the glass transition temperature. Below T_g it is more difficult to envisage such large scale movement but, nevertheless, evidence which suggests that this is possible has recently appeared for a number of polymers. In the case of amorphous PET, Yeh and Geil [Ref. 14] have shown by electron microscopy that small ball like structures, of diameter 45-100 Å, are present in the glassy solid and, significantly, that after 6 days at 60°C (5°C below T_g) these had rearranged into larger spherical aggregates of about 5 to 10 balls in diameter. As pointed out by Yeh and Geil, a 75 Å sphere would correspond to a single molecule with a molecular weight of about 100,000 and therefore, by comparison with the osmotic molecular weight of 15,000, is expected to comprise a small number of molecules. This suggests that it would be reasonable to adduce from these macroscopic movements evidence for large scale movements on a molecular scale which could account for the present results. It is to be hoped that further work will permit more quantitative comparisons between the two methods.

Decay of Radicals in Crystalline Samples. - The decay of radicals in polycrystalline samples was studied by following the decrease in height of the central peak of the first derivative spectrum with time of heating. At 100°C about 40% of the radicals survived after 10 hours and these decayed only slightly on further heating. At 120°C about 30% of the radicals were long-lived (Fig. 8). The decay did not conform to simple kinetics.

In contrast to the above findings, a simple first order decay of radical I was observed in specially treated samples of oriented crystalline polymer. A linear dependence of the logarithm of radical concentration on time of heating held for the decay of about 80% of the radicals at 100°C and for 95% at 120°C; the respective rate constants were 1.0×10^{-4} sec^{-1} and 2.7×10^{-4} sec^{-1} as shown in Fig. 9. These simple results were obtained only at the price of what, hopefully, may prove to be an unnecessarily complicated sequence of operations which were as follows:

1) Oriented films of PET were briefly exposed to air, for about 5 minutes, following γ-irradiation in a vacuum. The films were then thoroughly degassed and resealed in a vacuum. The rationalization of this process is that access of oxygen destroys free radicals in amorphous regions leaving a population predominantly of radical I along with radical II and the species giving the unassigned singlet in the crystallites (c.f. ref. 9).

2) The sample was heated at 160°C until radical I had decayed, after about one hour.

3) The sample was exposed to laboratory fluorescent lighting for several weeks during which time radical II was replaced by radical I by a photochemical reaction [Ref. 15].

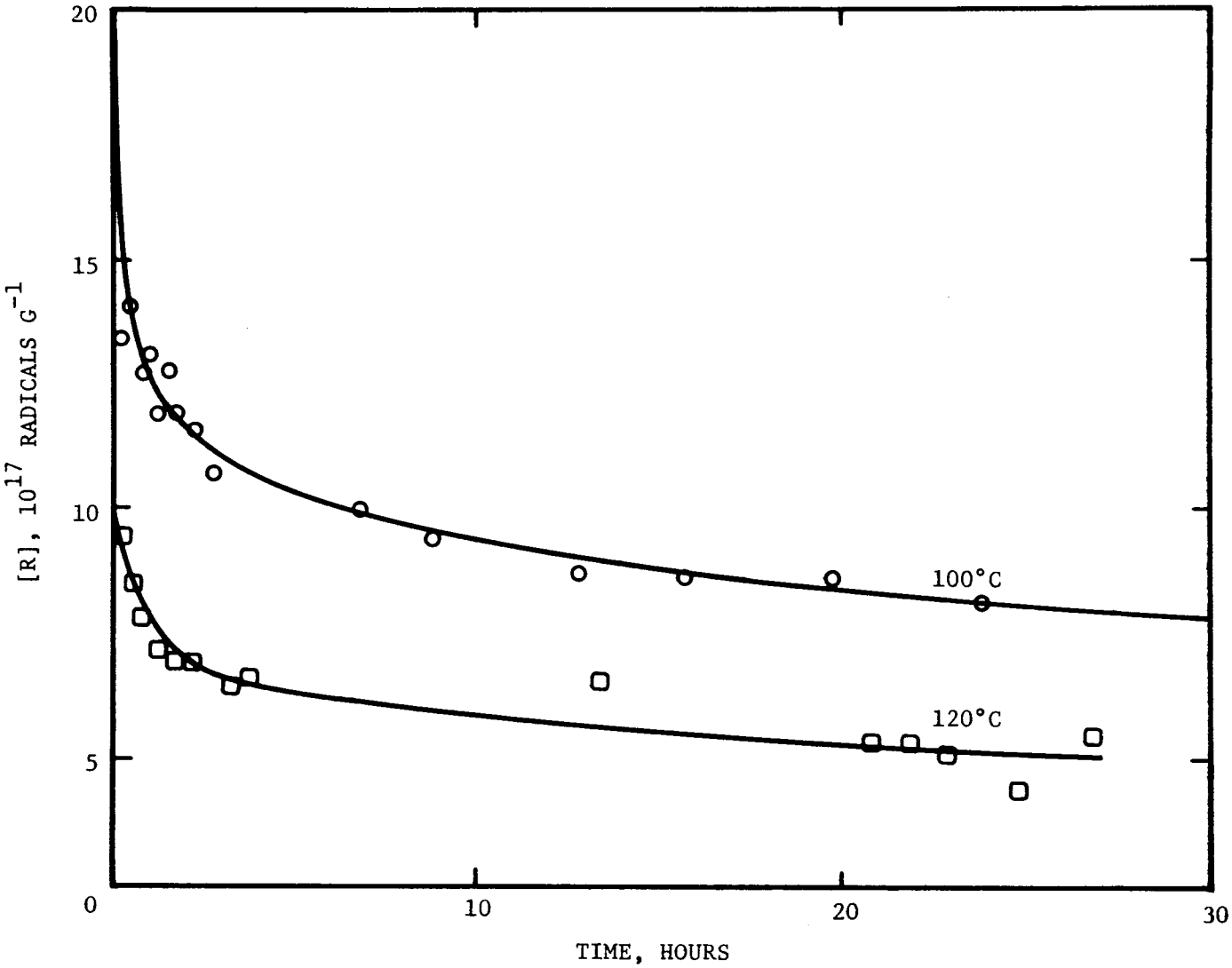

Figure 8. DECAY OF RADICALS IN POLYCRSTALLINE SAMPLES OF POLY(ETHYLENE TEREPHTHALATE)

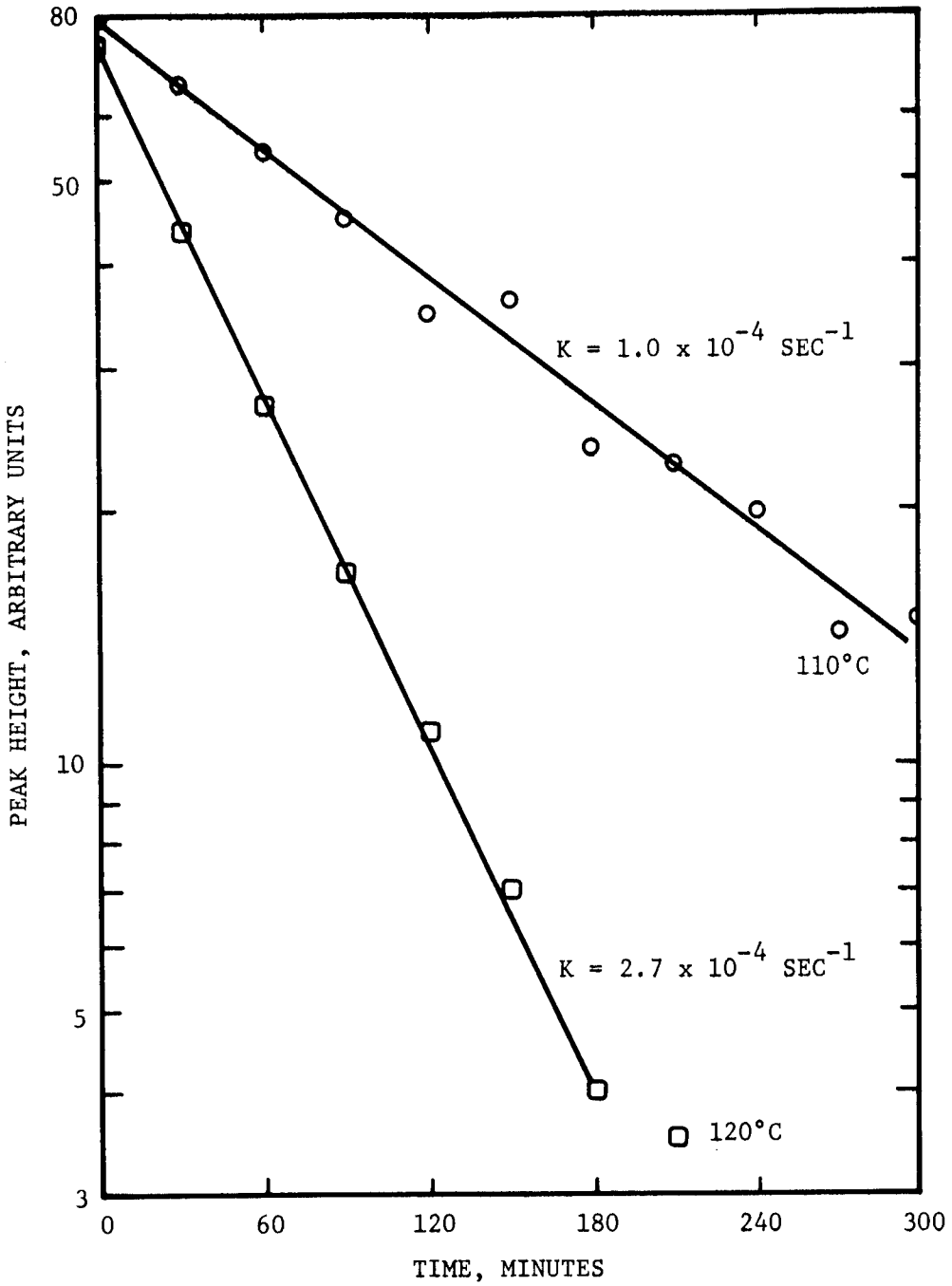

Figure 9. FIRST ORDER PLOTS FOR DECAY OF TYPE I RADICALS IN ORIENTED CRYSTALLINE POLY(ETHYLENE TEREPHTHALATE).

The population of radical I generated in the above way gave the usual well resolved ESR spectrum, 6 or 8 lines depending on orientation in the magnetic field [Ref. 9]. The decay was followed by reference to the heights of outer peaks which have the advantage of being clearly separated from central components of the spectrum. Similar results were obtained by reference to peaks 1 and 2 of both six and eight line spectra (c.f. ref 9). During this decay the central portion of the spectrum did not change significantly and it is concluded that radical I disappears largely by bimolecular reactions rather than by conversion into other radical species.

In order to account for first order kinetics it is suggested that the rate determining step is the movement of a radical site to the surface of a crystallite. At the surface, the radical is supposed to react rapidly with similarly situated radicals in other crystallites which are moving freely in an amorphous matrix 30°C, or more above T_g. The smallest dimension of a crystallite in PET is 100-200 Å [Refs. 16, 17] and the question remains of how radicals could move over such distances in a crystalline medium. Reference to the high melting point of the polymer, about 255°C, suggests that long range segmental displacements are unlikely to be important at temperatures as low as 110°C. In these circumstances, it would appear reasonable to adopt the hypothesis of the migration of free radical sites by hydrogen atom hopping [Refs. 2, 3, 4]. Moreover, consideration of atomic arrangement in crystalline PET would suggest that such hopping would follow prescribed routes along isolated stacks of $-CH_2-CH_2-$ groups which would tend to minimize bimolecular reactions of radicals within the crystallites.

SECTION III

POST IRRADIATION ELECTRICAL PROPERTIES

3.1 Post Irradiation Conductivity of Poly(ethylene terephthalate)

Conductivity of Poly(ethylene terephthalate). - It is well known that exposure of a polymer to ionizing radiation may result in an increase in electrical conductivity even after removal of the sample from a radiation field [Ref. 18]. The usual explanation of this post-irradiation conductivity is that it is due to the release of positive and negative charges which are trapped during irradiation. An alternative suggestion made by Tal'rose and Frankevich is that charge carriers are generated in post-irradiation reactions of free radicals [Ref. 19]. Experimental evidence for this unusual suggestion was adduced from studies of a sample of a paraffin, mpt-52-55°C, which had been irradiated in the solid state under nitrogen with high energy electrons; a correlation was reported between radical decay, followed by monitoring the electron spin resonance signal of the radical $-CH_2-\dot{C}H-CH_2-$, and a peak in conductivity as the sample was warmed. Further studies of this kind would be desirable to check more closely whether charge carriers can be generated by the reaction of free radicals. Verification requires post-irradiation conductivity data for polyethylene terephthalate for comparison with previously documented data on the kinetics of free radical disappearance.

Experimental. - Sheets of completely amorphous (10 mils) and partially crystalline samples of biaxially oriented (1 mil) PET were provided with aluminum (830 Å) or silver (300 Å) electrodes by vacuum evaporation. Samples were thoroughly degassed and exposed in nitrogen to Co-60 γ-rays.

The effect of an applied bias during irradiation was investigated and air was substituted for nitrogen to determine the effects of oxygen in the environment. External circuitry was applied to the sample through pressure contacts against the evaporated electrodes. Bias conditions were normally 100 volts/mil. The sample holder for irradiation and current measurements is shown in Fig. 10.

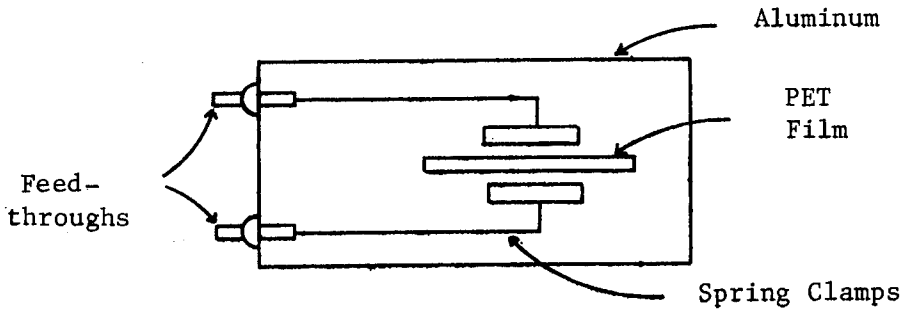

Figure 10. SAMPLE HOLDER FOR γ-IRRADIATION MEASUREMENTS.

Figure 11 shows the experimental results for a 1 mil sample. Between 4 and 20 Mrads the conductivity is seen to increase linearly with dose. This can be compared to the accumulation of free radicals in Fig. 4. A direct relationship at this point would give 8×10^{-11} amperes for about 5×10^{17} radicals per gram. This corresponds to 5×10^{-12} charge carriers per free radical giving an energy level for the radical site of 0.65 eV below the conduction level or above the valence level if one assumes a mobility of $10^{-3} cm^2 v^{-1} sec^{-1}$. Since a band model is not expected to be valid for such a low mobility, this is a rough approximation.

Similar results are shown for 10 mil samples in Fig. 12. Up to about 35 Mrads the response may have been damped by the presence of some residual oxygen or other contaminant in the system. Both samples were purged with nitrogen at this point followed by a continuation of the irradiation. The sample which was irradiated without a bias exhibited a much more rapid increase in conductivity. This behavior would indicate polarization or some type of trapped charge accumulation. In order to characterize this effect, decay curves of conductivity were obtained under various conditions. The procedure consisted of terminating the irradiation, moving the sample to an adjacent room, applying a voltage and monitoring the current passing through the sample. A time delay of 1 to 30 minutes occurred between termination of irradiation and applying the sampling voltage. The time origin of the following graphs corresponds to the time of voltage application.

The current decay of a 10 mil PET sample on which voltage was applied during irradiation is shown in Fig. 13 for 2 different dose levels. After the first two minutes the decay follows first order kinetics with a decay constant of $2.6 \times 10^{-4} sec^{-1}$. Figure 14 is a similar plot for a sample on which no voltage was applied. The slope is steeper for this sample indicating that the decay of this additional component is voltage dependent.

Conductivity buildup was reduced by 3 or 4 orders of magnitude in the presence of oxygen. Figure 15 shows the post irradiation current in 10 mil PET irradiated in air. The early part of these curves appears to be the normal polarization response. Near the end it has about the same slope as the curve of Fig. 14. This may be the result of free radicals deep in the sample which oxygen has been unable to reach.

Similar results were obtained for a 1 mil PET sample. In Fig. 16 the decay is followed for 100 minutes where it appeared to stabilize or at least decay with a much longer time constant. With this component subtracted out, the resulting curve has a constant slope within experimental error. This latter curve is plotted using the right hand scale. At this point in time the above sample was studied further in the manner described for the experiments in the following section.

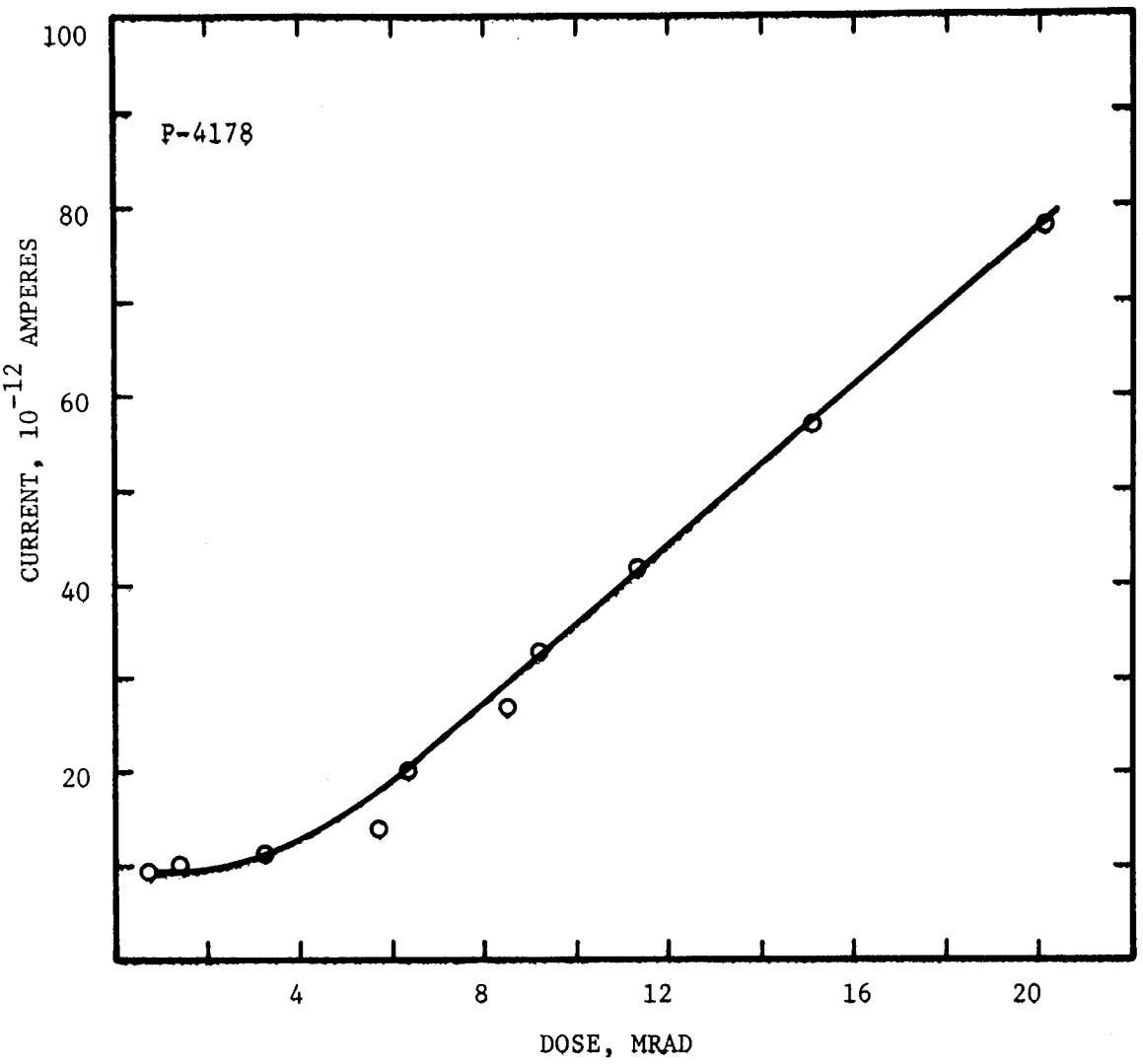

Figure 11. CURRENT IN 1 MIL PET AS A FUNCTION OF ACCUMULATED γ-DOSE.

Applied voltage during and after
irradiation = 100 volts, 300 Å silver electrodes
with area = 3.88 cm^2,
dose rate = 0.038 Mrad hr^{-1}.

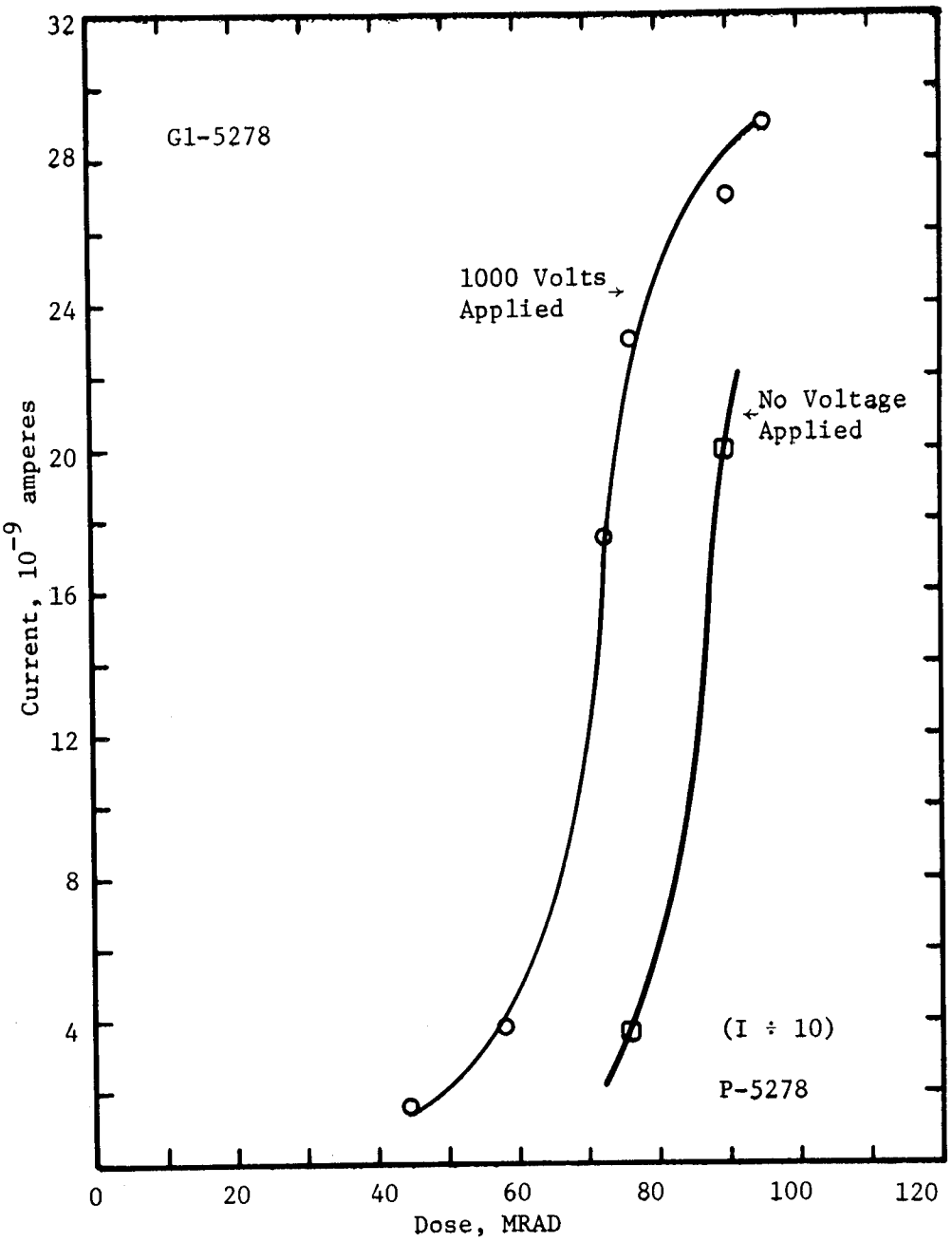

Figure 12. CURRENT IN 10 MIL PET AS A FUNCTION OF THE ACCUMULATED γ-DOSE. Applied voltage = 1000 volts, area = 3.88 cm^2, 830 Å aluminum electrodes, dose rate = 0.19 Mrad hr^{-1}, O···1000 volts applied during irradiation, □···no voltage applied during irradiation.

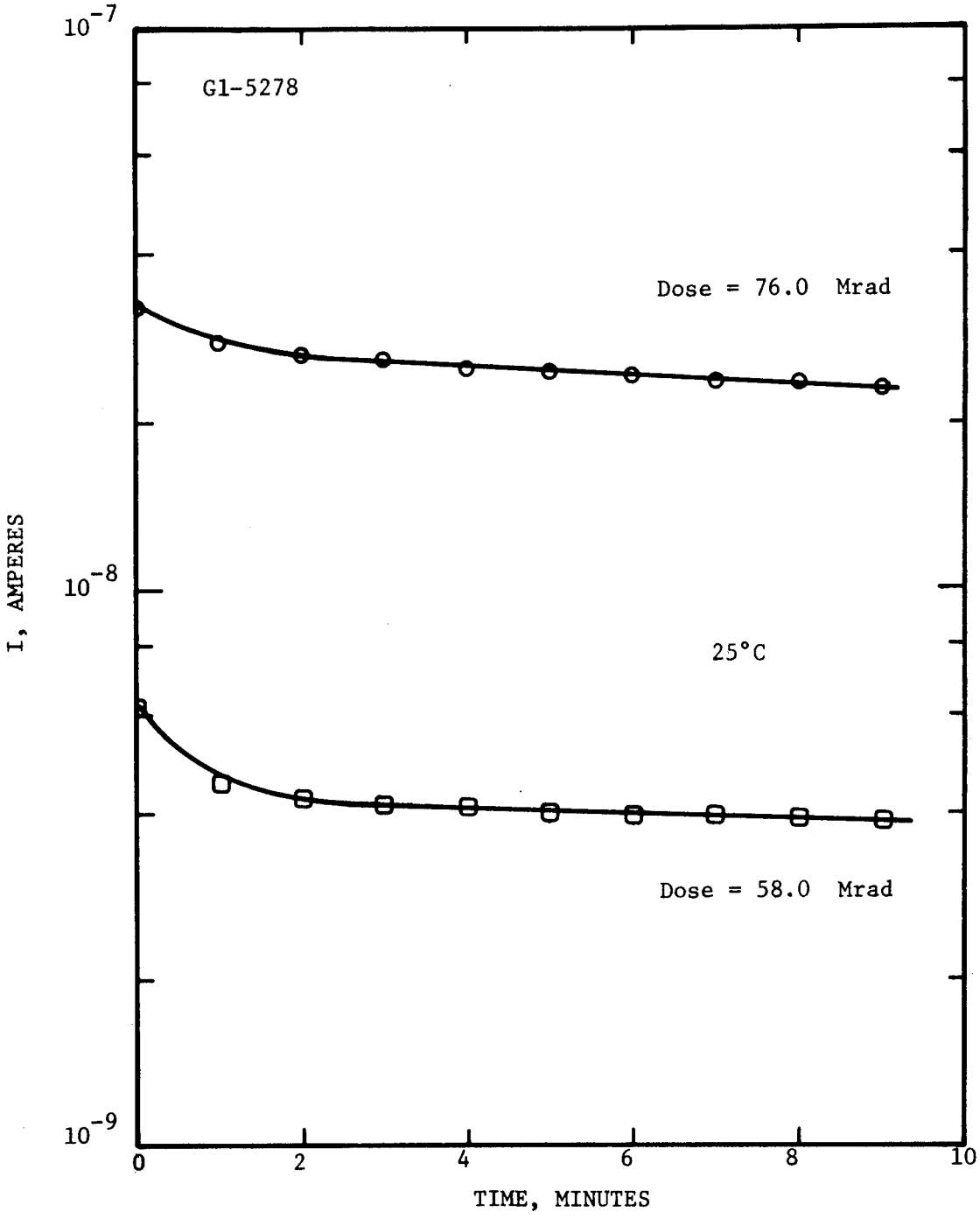

Figure 13. FIRST ORDER CURRENT DECAY OF 10 MIL PET IRRADIATED IN N_2. 1000 volts applied during irradiation, applied voltage during current measurements = 1000 volts

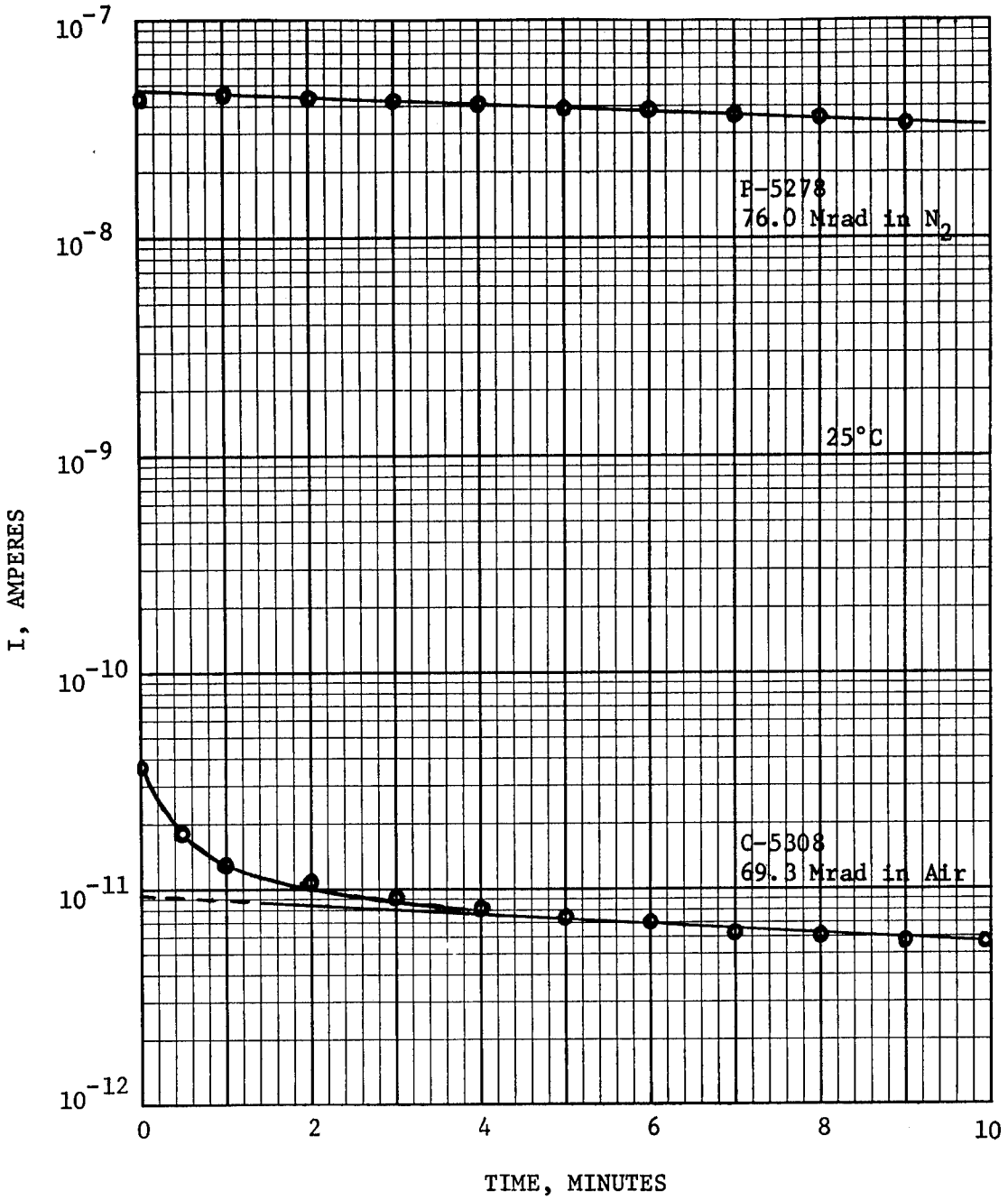

Figure 14. COMPARISON OF FIRST ORDER CURRENT DECAY OF 10 MIL PET IRRADIATED IN N_2 AND IN AIR. No voltage applied during irradiation, applied voltage during measurement = 1000 volts.

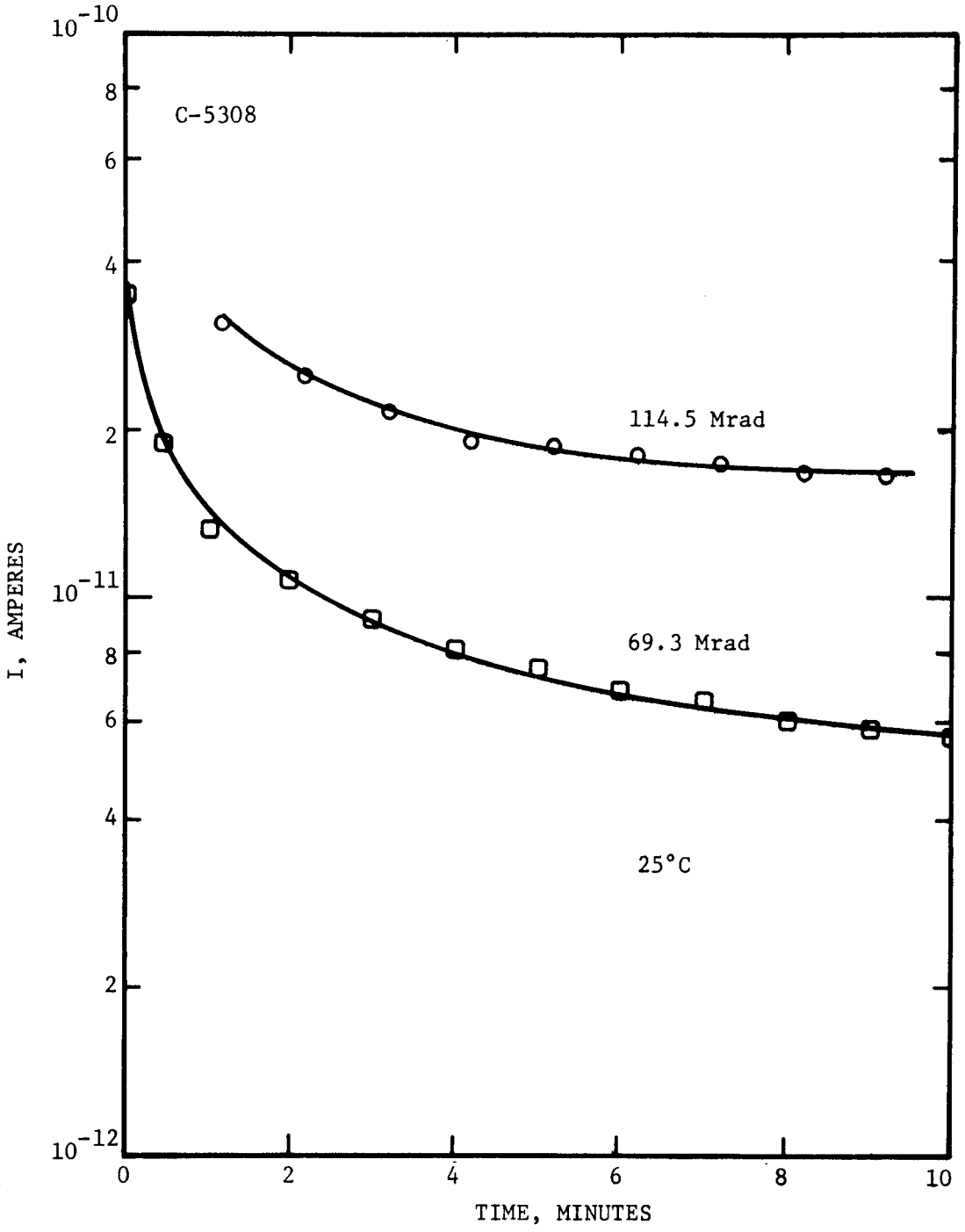

Figure 15. FIRST ORDER CURRENT DECAY OF 10 MIL PET IRRADIATED IN AIR. No voltage applied during irradiation, applied voltage during current measurement = 1000 volts

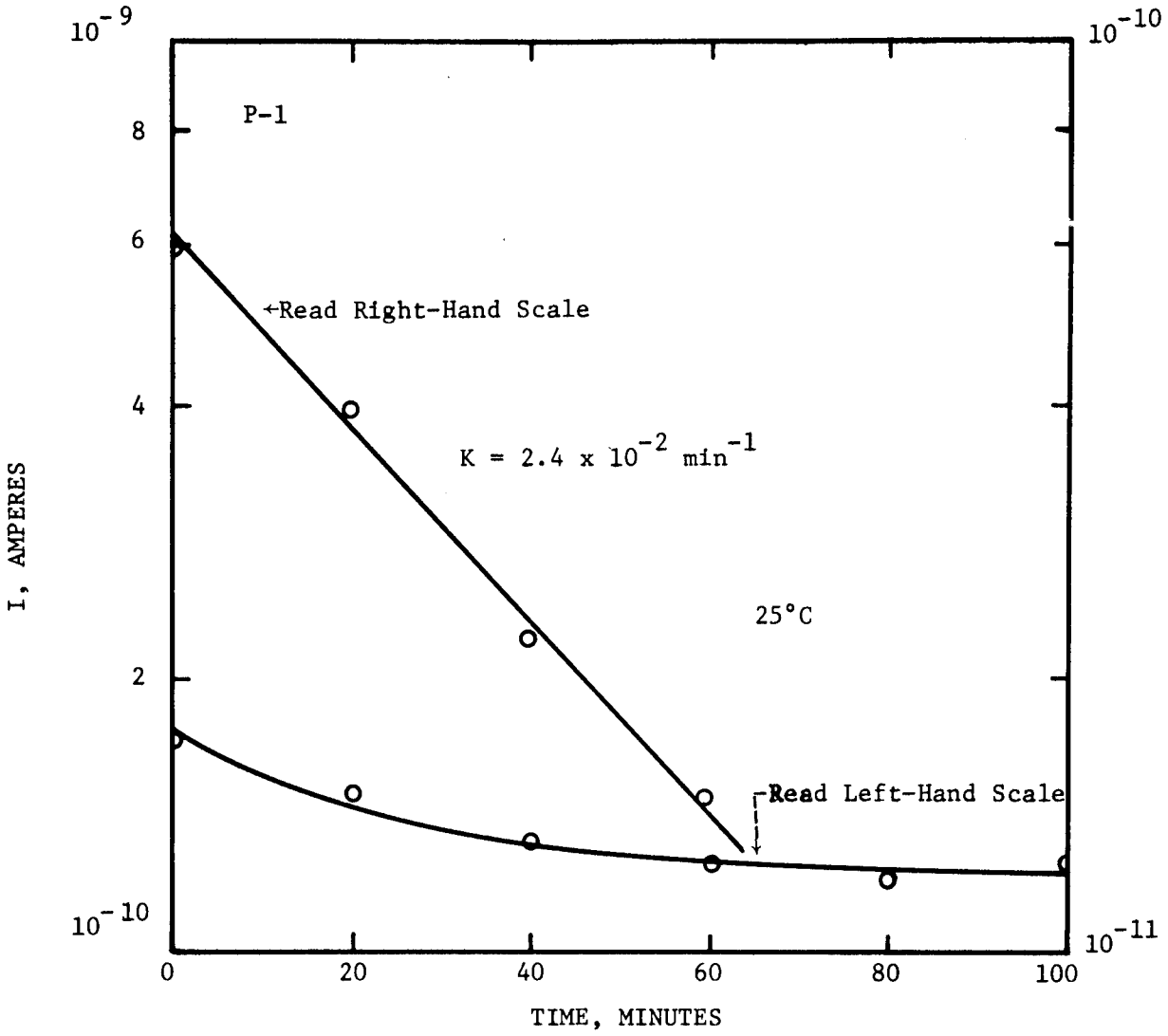

Figure 16. FIRST ORDER CURRENT DECAY IN IRRADIATED 1 MIL PET.
V = 100 volts
300 Å aluminum electrodes with area = 3.88 cm^2
Dose = 6 Mrad

3.2 Charge Release and Conductivity Decay Kinetics of Irradiated PET

For these experiments a sample holder was used which was similar to that described in Sec. 3.1. For the various periods of irradiation the current was monitored in each sample as the temperature was increased at a constant rate. The rate is indicated by $\frac{dT}{dt}$. The result of this experiment was dependent upon the amount of dose received, but the background current observed was often the dominating factor.

Figure 17 shows the results for the 1 mil sample which was allowed to decay earlier at room temperature. A peak in the current was observed at 115°C. Of all samples observed in this manner, a peak or anomaly in the current was observed between 110°C and 130°C. Samples of 10 mil PET irradiated at a relatively low dose level are also shown. It is expected that samples irradiated at higher levels might have shown a peak similar to that seen in the 1 mil sample. A lower voltage may also bring out the peak. As demonstrated with sample P-6288, several days annealing at 80°C appears to remove the peak. For comparison, an unirradiated sample is shown in Fig. 18. The current observed without bias is very small but it does indicate the characteristic peak.

Since the decay characteristics of free radicals had been obtained earlier, this seemed to offer a technique of correlating the free radical concentration to the conductivity of PET and possibly verify or deny the relation suggested by Talrose and Frankevich. To obtain this information a sample of 10 mil PET with a large post irradiation conductivity was held at 73.5°C,and the current monitored for over 500 minutes. The second order kinetics of the current decay are shown in Fig. 19. The sample temperature was then raised to 77.0°C and the current monitored for another 500 minutes and plotted in Fig. 20. The decay constant is seen to increase considerably. For comparison these 2 values of the decay constant were placed on an Arrhenius plot in Fig. 21 as was done for the ESR free radical decay data. The activation energy of 101 Kcal $mole^{-1}$ compares well with the 112 Kcal $mole^{-1}$ obtained for the free radical decay constants. This information is very significant; however, more data should be obtained to substantiate the two points. Later experiments with samples having a low irradiation dose were dominated by background currents. These results are plotted on the same figure. Very little additional information can be obtained from this upper curve but it demonstrates the need for observing the various electronic processes under the proper conditions of temperature and radiation history.

Current decay characteristics of the polycrystalline samples is shown for a 1 mil sample at elevated temperatures in Fig. 22. The time constant is very long at each temperature for which decay was observed. The procedure consisted of observing the current for several hours at the lowest temperature then raising the temperature to the next value. It is possible that the temperatures are near enough that the decay at the higher temperature is altered by the previous history at the lower temperature. Also a different result may be obtained if the residual current of each temperature were subtracted from the data. This was done at 123°C. Within experimental error a first order decay is seen with a decay constant of 2.3×10^{-3} min^{-1}.

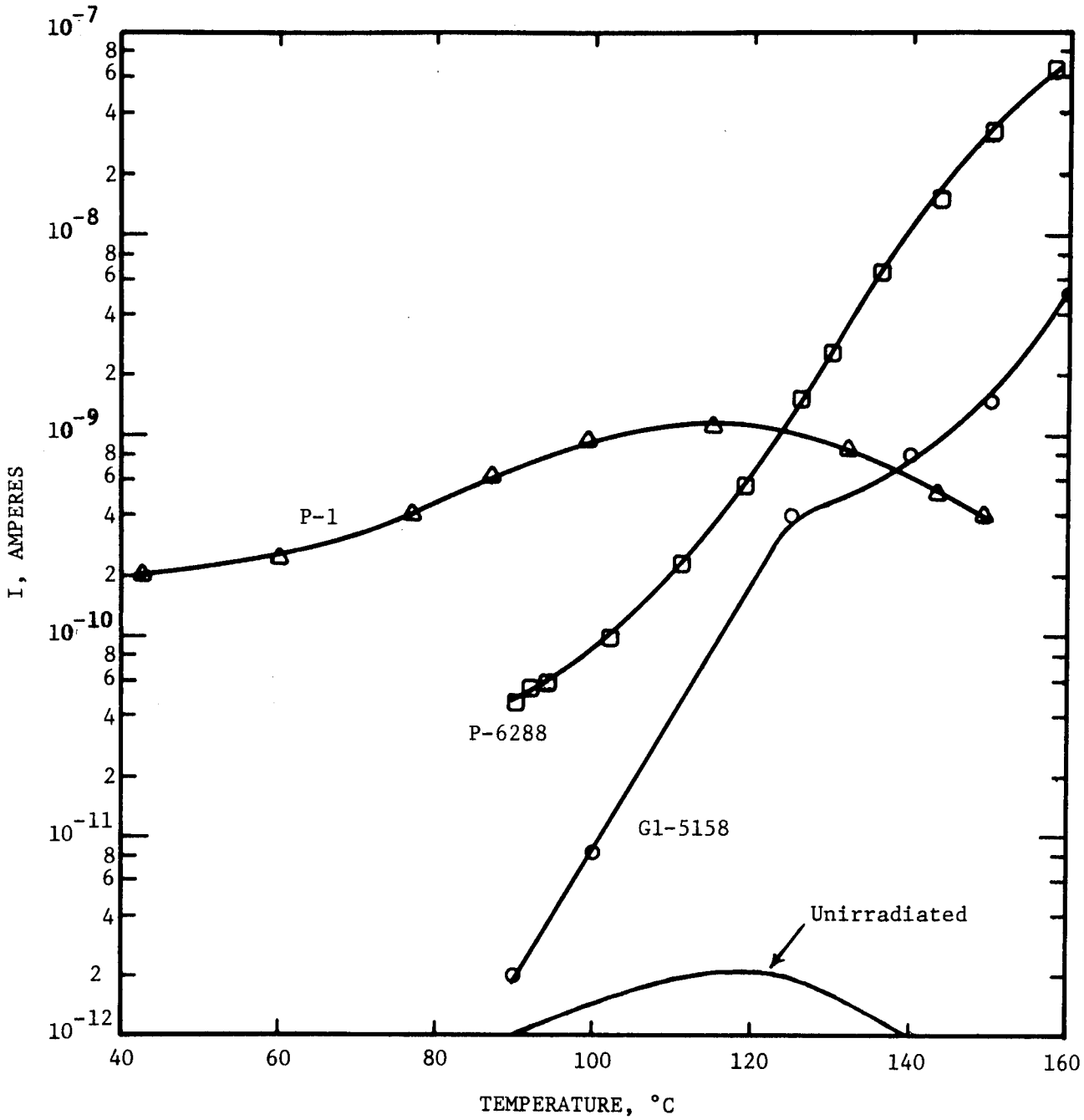

Figure 17. CONDUCTION CURRENT VERSUS TEMPERATURE IN PET UNDER TRANSIENT TEMPERATURE CONDITIONS.

Δ- - - 1 mil, dT/dt = 4.2°C/min, 300A° silver electrodes - 3.88 cm^2, V = 100 volts, Dose = 6.0 Mrad.

O- - - 10 mil, dT/dt = 5.0°C/min, 300A° silver electrodes - 3.88 cm^2, V = 2000 volts, no irradiation.

□- - - 10 mil, dT/dt = 2.0°C/min, 830A° aluminum electrodes - 3.88 cm^2, V = 1000 volts, Dose = 10-20 Mrads, sample was held near 80°C for several days before taking measurement.

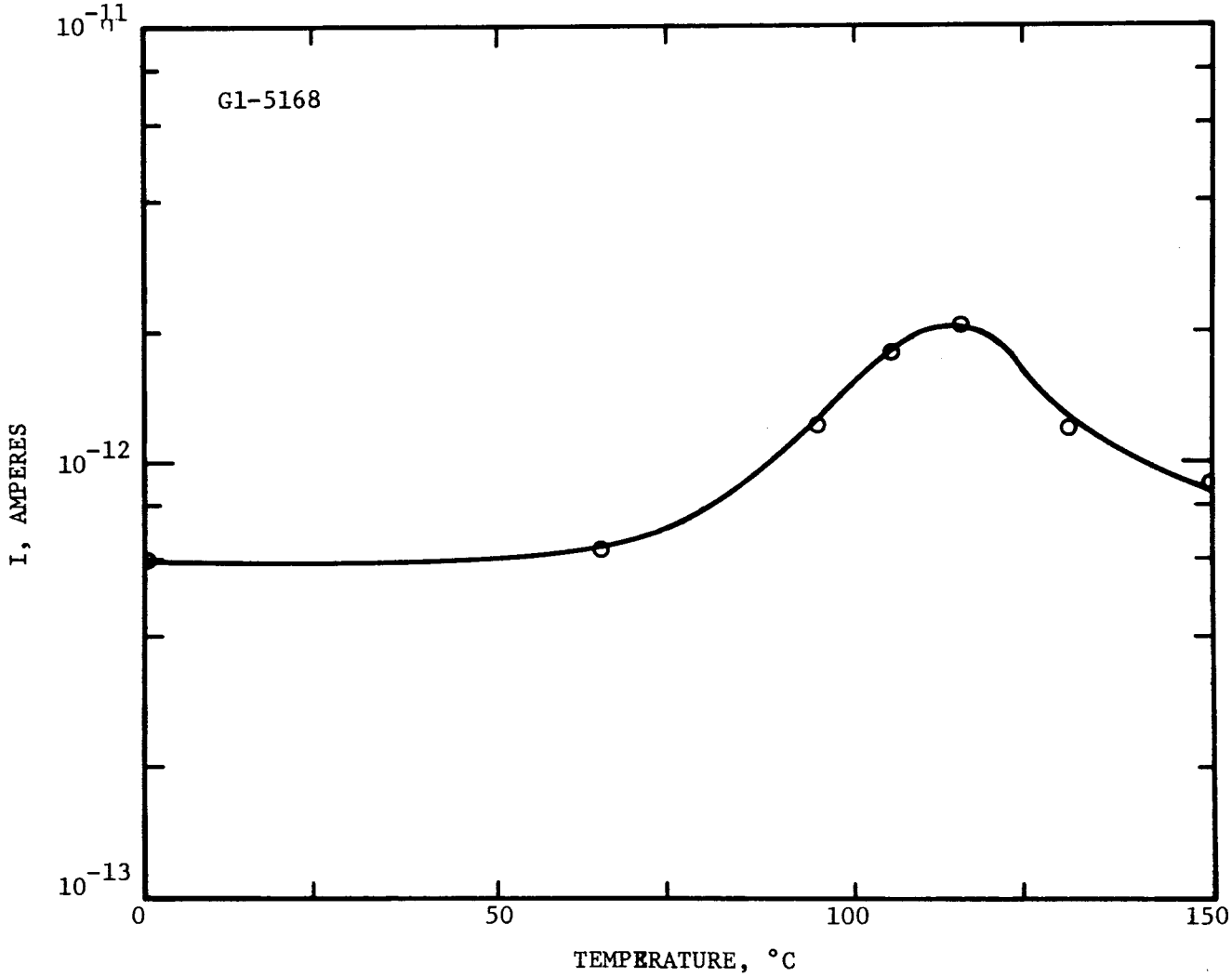

Figure 18. TRANSIENT CURRENT VERSUS TEMPERATURE IN 10 MIL PET. No voltage, no irradiation, dT/dt = 5.6°C/min 300 Å aluminum electrodes with area = 3.88 cm^2

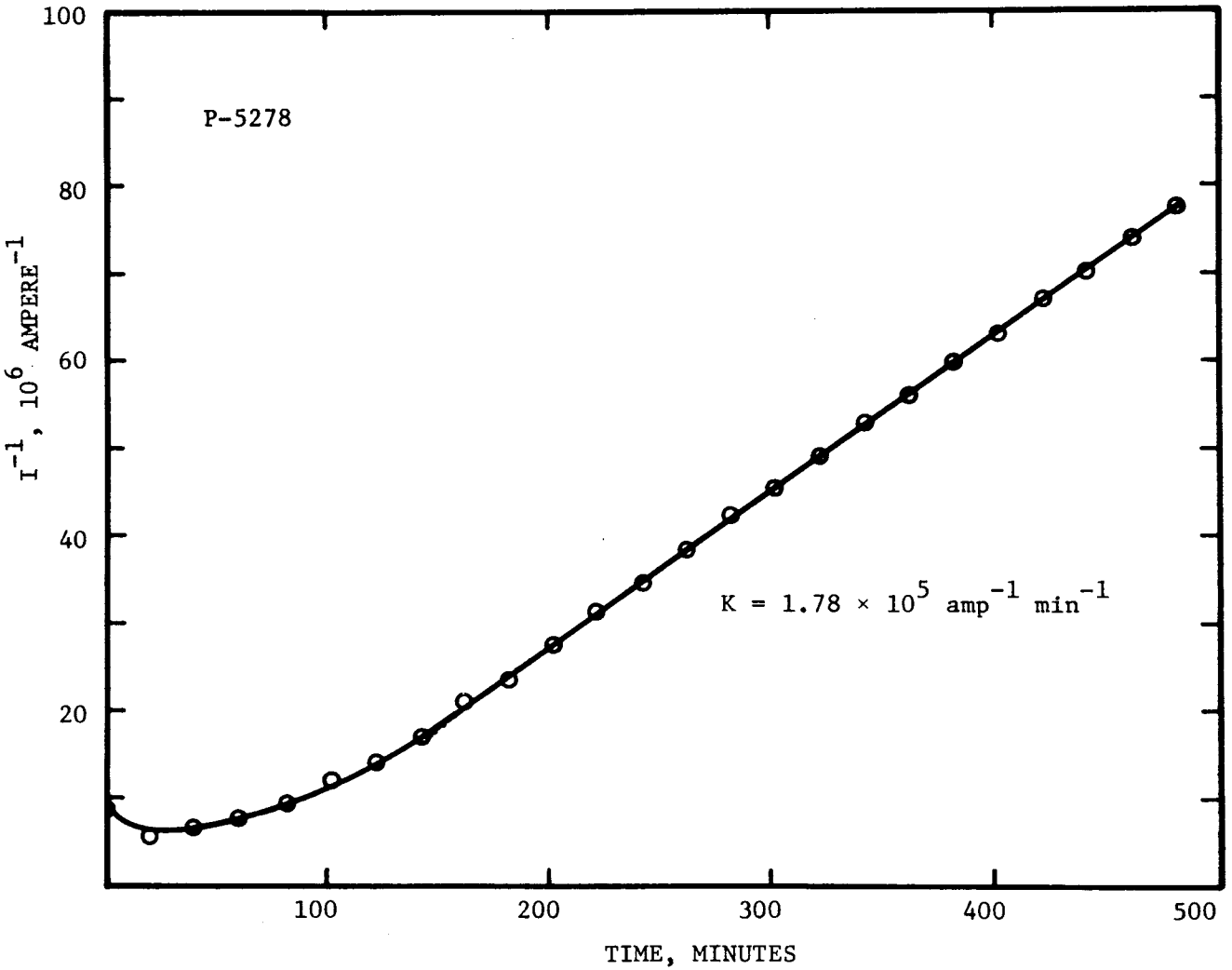

Figure 19. SECOND ORDER CURRENT DECAY IN 10 MIL PET.
Applied voltage = 1000 volts, 830 Å aluminum electrodes with area = 3.88 cm^2
Temperature = 73.5°C

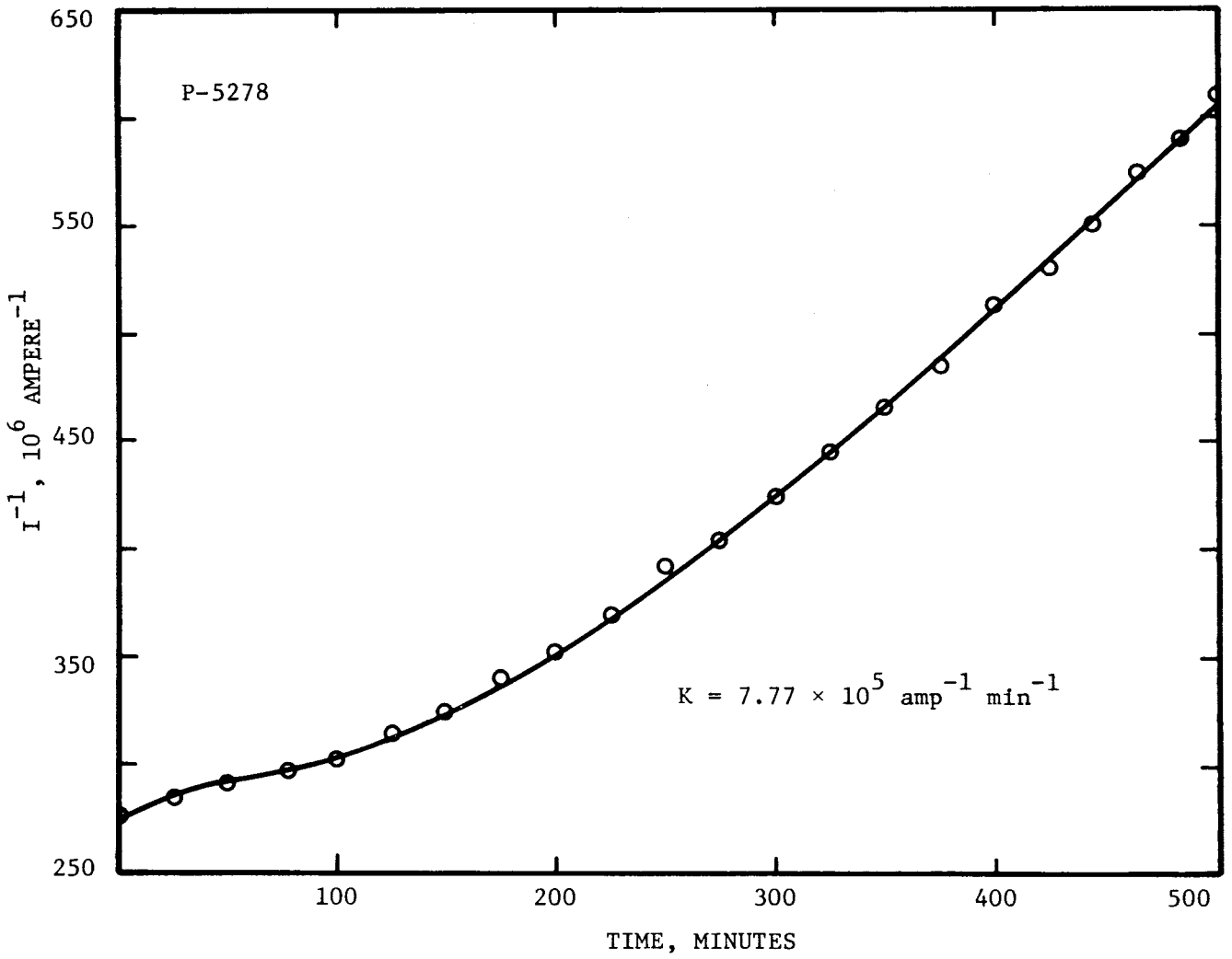

Figure 20. SECOND ORDER CURRENT DECAY IN 10 MIL PET.
Applied voltage = 1000 volts, 830 Å aluminum electrodes with area = 3.88 cm^2
Temperature = 77.0°C

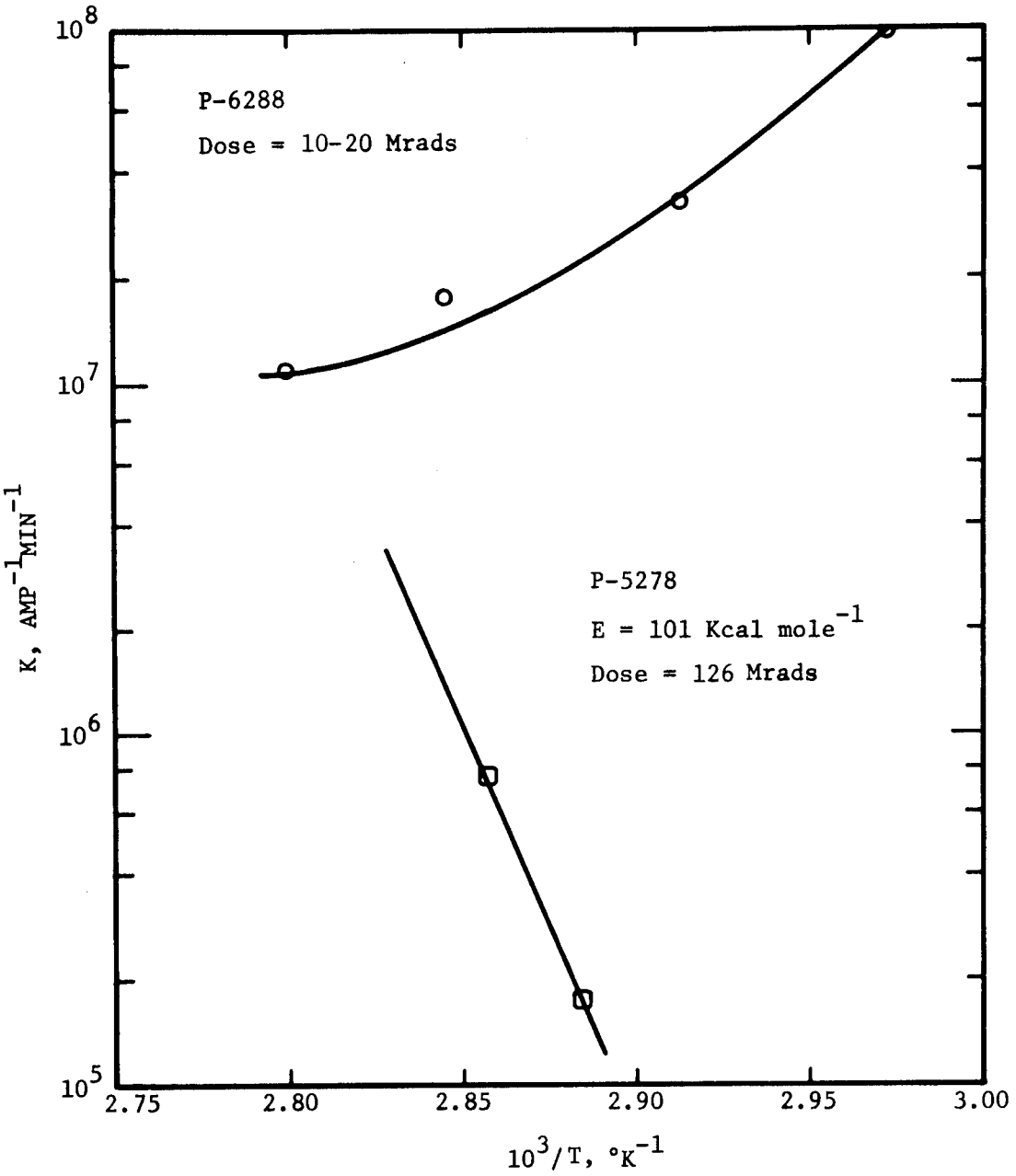

Figure 21. ARRHENIUS PLOT FOR THE SECOND ORDER DECAY CONSTANTS FOR CONDUCTIVITY IN 10 MIL PET.

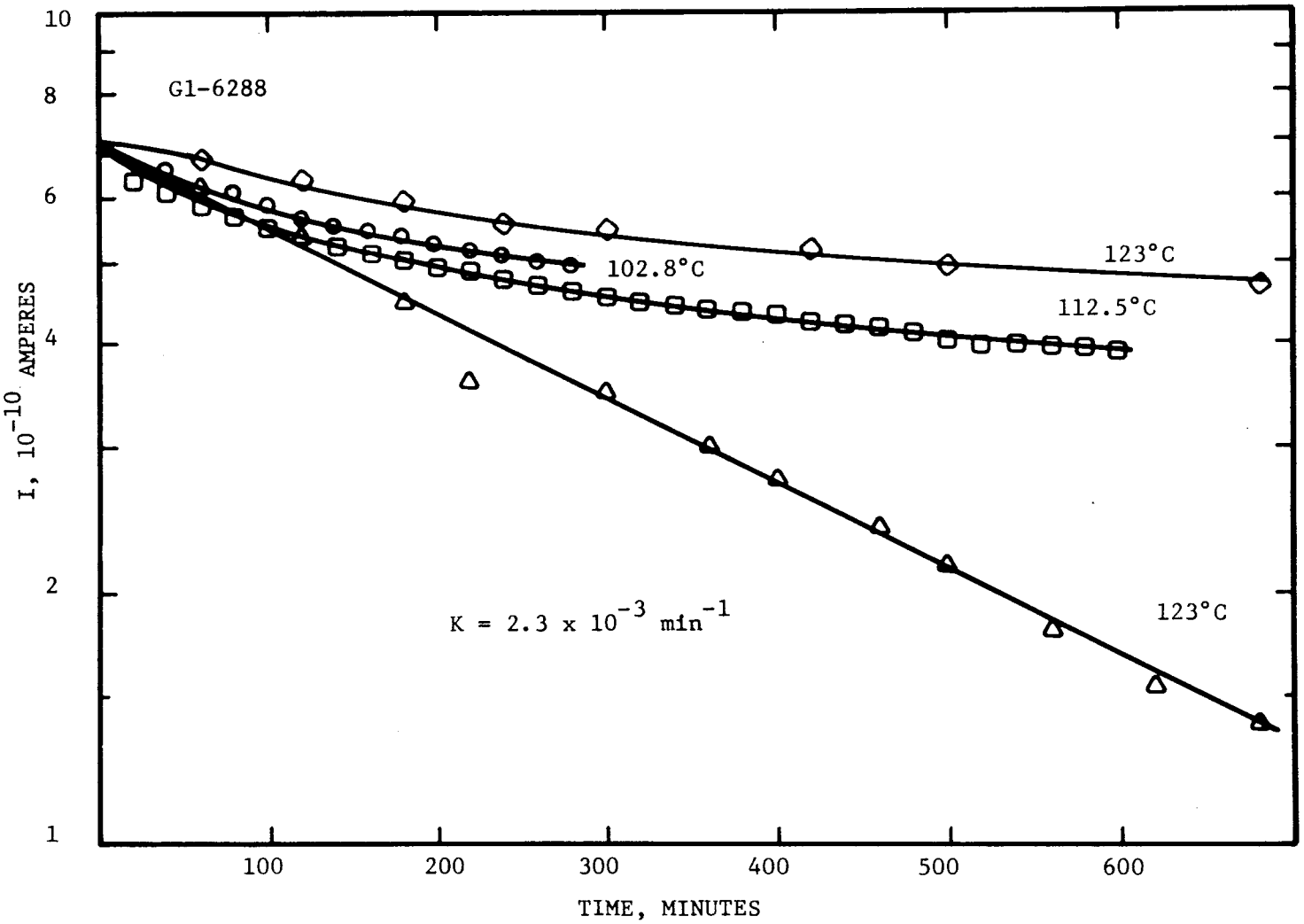

Figure 22. FIRST ORDER CURRENT DECAY IN 1 MIL PET.
(normalized to same zero points)
Applied voltage = 100 volts
◇- - - steady state value included,
△- - - after subtracting steady state value.

3.3 Transit Time Measurements

3.3.1 Technique

Transit time measurements have been approached from several techniques in terms of samples used, experimental setup, and method of evaluation. The samples used have been dimethylterephthalate (DMT), dibenzoate ester of ethylene glycol (DEG), and PET. Carrier generation has been initiated both by X-ray pulse and xenon flash lamp. Electrodes have included 300 Å silver and tin oxide on glass, and sodium chloride solutions. For X-ray pulses 800 Å of aluminum as well as 300 Å of silver have been used. 300 Å silver was necessary for the xenon flash lamp experiments in order to allow transmission through the electrode of the near u-v photons. However, silver electrodes gave evidence of migration and loss of contact. The current response to the excitation pulse was monitored on an oscilloscope and recorded photographically. Two techniques in analyzing these pulses were used. The first technique is a time of flight technique where the transit time is the time between initiation and the peak of the pulse. The second technique is an integrating procedure especially desirable when the carrier lifetime is shorter than the true transit time. In this technique one uses the height of the integrated pulse as well as the initial slope of the pulse to obtain the true transit time and the carrier lifetime.

The experimental arrangement is shown in Fig. 23. Photon excitation is accomplished by passing the light pulse through a semitransparent electrode on which a voltage is applied. X-ray excitation is accomplished by a collimated beam from the side. The slit width is approximately 1/10 the length (L) of the sample. The arrangement for using tin oxide electrodes on glass is shown in Fig. 24. Adjustable clamps were used to apply pressure to the glass to hold the electrodes in position. Success of this technique depends upon having flat surfaces and in aligning the tin oxide surface and the crystal face. Only the xenon lamp pulse was used with the tin oxide electrodes. The circuitry for recording the current pulse is shown schematically in Fig. 26.

The capacitance C is the cable capacitance between the sample holder and the oscilloscope which monitors V_o. V_o is related to the current pulse by

$$I = C \frac{dV_o}{dt} + \frac{V_o}{R} \quad . \tag{3.1}$$

For a very small value of R one gets a real time output pulse

$$V_o = IR \quad . \tag{3.2}$$

For a very large value of R one gets an integrated output

$$V_o = \frac{1}{C} \int I dt. \tag{3.3}$$

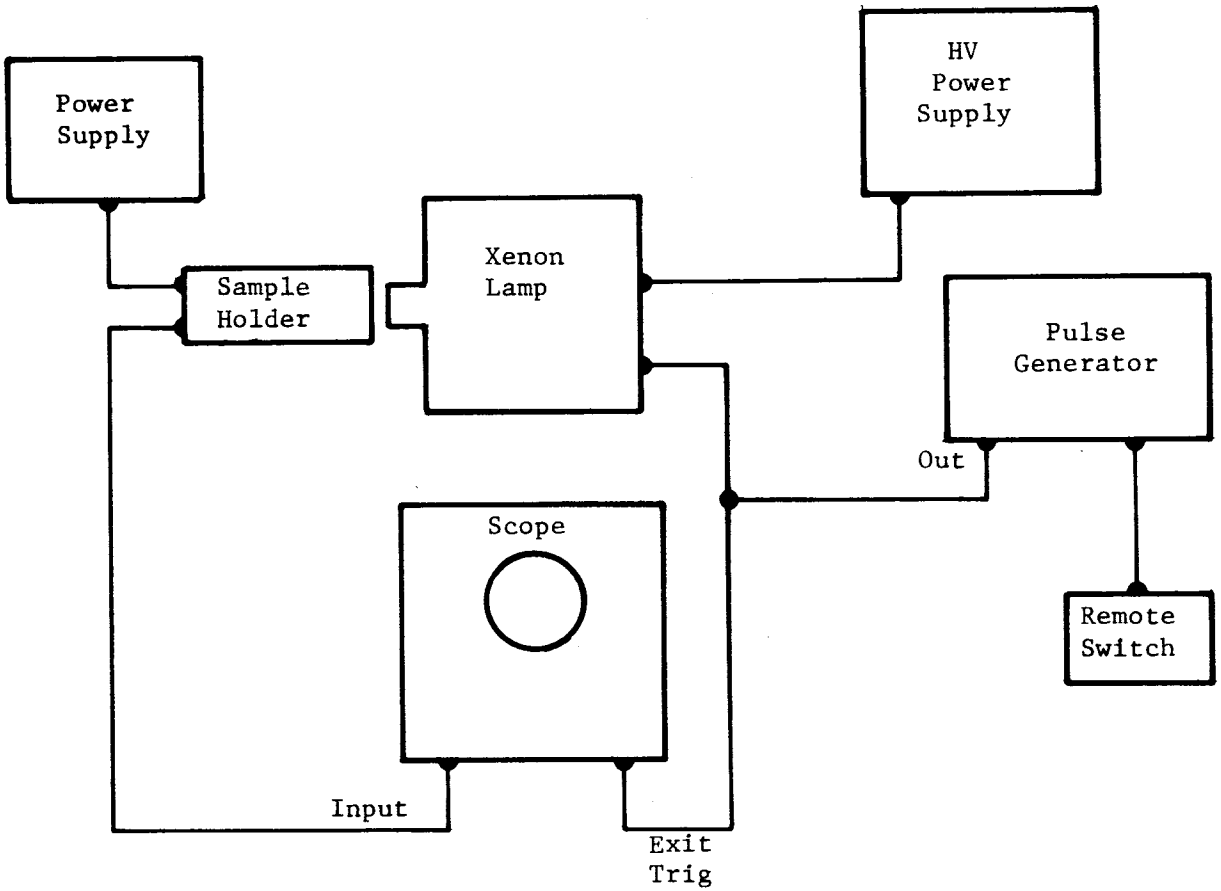

Figure 23. EXPERIMENTAL TECHNIQUE FOR TRANSIENT PHOTORESPONSE MEASUREMENTS.

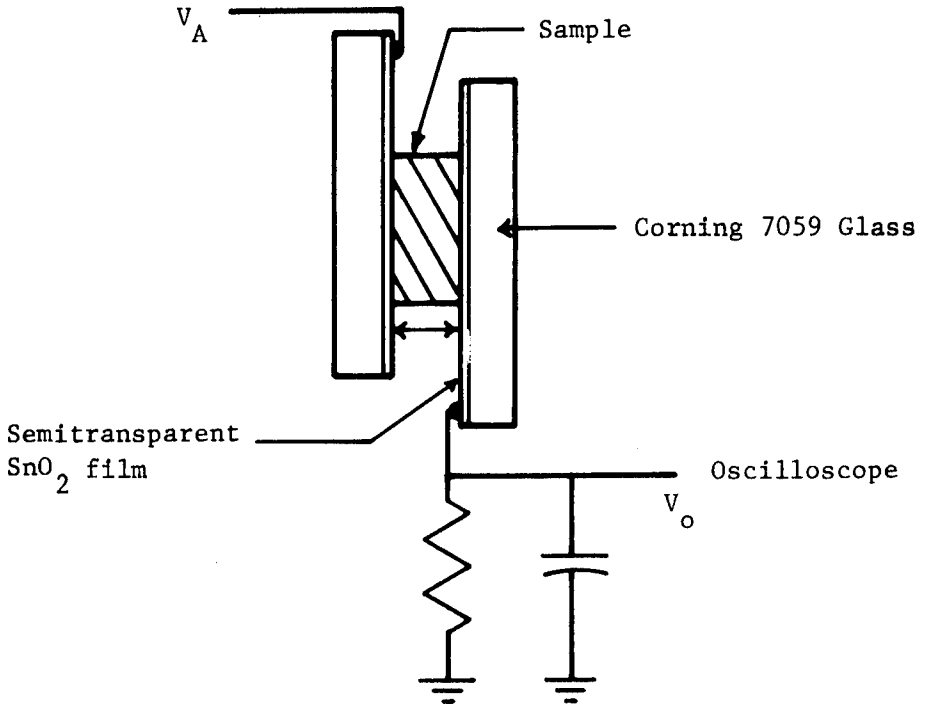

Figure 24. TRANSIT TIME TECHNIQUE USING SnO_2 ELECTRODES.

When the carrier lifetime is short, the real time photocurrent peak does not correspond to the true carrier transit time. Movement of the peak as the applied voltage varies may be so slight as to be unobservable. When integrated such a pulse looks like the curve shown in Fig. 25. Analytically, the slope of the output voltage curve at the origin is extrapolated upward until it intersects the voltage line corresponding to total collection of the generated charge. This point of intersection, t^1, is the effective drift time. Seitz [Ref. 20] has shown that the variation of the effective drift time with voltage can be used to calculate both the carrier lifetime and the true transit time. This relation is given by

$$\frac{\tau_n}{t^1} = [1 - \exp(-T_{tr}/\tau_n)]^{-1} \qquad (3.4)$$

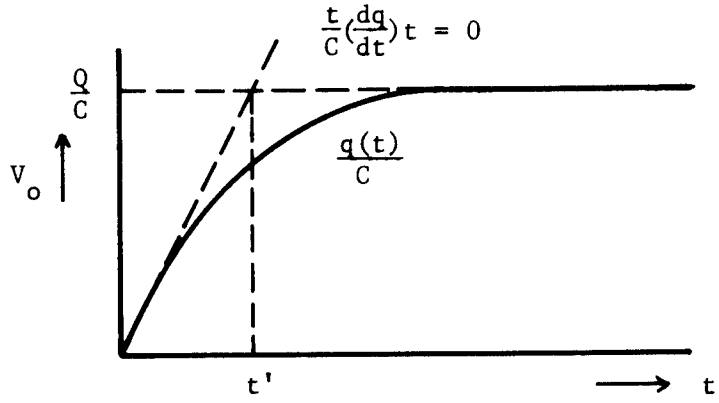

Figure 25. OUTPUT VOLTAGE OF INTEGRATING CIRCUIT WHEN THE CARRIER LIFETIME IS SHORT.

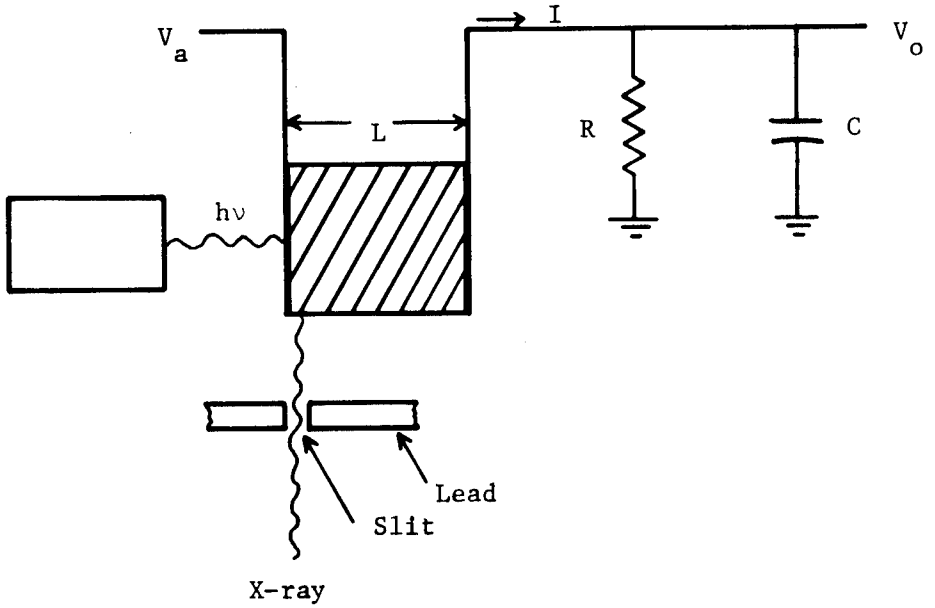

Figure 26. EXPERIMENTAL ARRANGEMENT SHOWING PHOTON AND X-RAY EXCITATION OF CARRIERS AND THE CURRENT MONITORING CIRCUIT.

where the true transit time is defined in terms of the drift length L, drift mobility μ, and the applied voltage V_a

$$T_{tr} = \frac{L^2}{\mu V_a} \tag{3.5}$$

The above relationship is plotted in Fig. 27. When $T_{tr} < \tau_n$ only a small difference is observed between t' and T_{tr}. However, when $T_{tr} > \tau_n$, t' remains very near the value of τ_n. It is unfortunate that the sensitivity of this technique is lowest in the region where its use is somewhat mandatory.

3.3.2 Mobility of Dimethylterephthalate (DMT)

The relationship between DMT and PET is apparent in the two structural formulas:

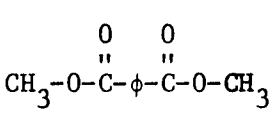

DMT

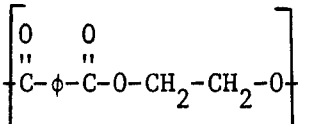

PET

The integrating technique as well as the real time technique was used to measure carrier mobilities along several axes. In most cases carrier lifetimes were longer than 1/2 millisecond and consequently the classical transit time pulses as described by Kepler were observed [Ref. 21]. Some typical pulses are shown in Fig. 28 and Fig. 29. A component of the pulse in the opposite direction of the applied voltage was observed in this sample as well as several other samples. Two explanations are possible for this behavior. Electrons may be ejected from the negative electrode by photons or X-rays. Or alternatively the electrode may be involved in a surface polarization which is neutralized by the excitation pulse.

Calculated mobilities for this compound are given in Table I. Much of the evidence upon which to decide the validity of these values lies in the manner in which the transit time or the effective drift time varies with voltage. In Fig. 30(b) the inverse relation which is expected for the trap free cases is observed. The height of the output pulse is nearly linear with applied voltage in Fig. 30(a). Results for a different crystal which was grown in this laboratory are shown in Fig. 31. Here the space charge limited current is observed or at least the current varies approximately as the square of the voltage. Transit time variation with voltage is shown in Fig. 32. The electron mobility for this crystal and the hole mobility along the c-axis were obtained from crystals grown from the same batch. Orientation measurements were not made on the crystals but the shortest crystal dimension was assumed to be the a-axis and the longest was assumed to be the c-axis. All other measurements were made using samples cut from the same boule and the orientation was determined by X-ray diffraction. These samples were obtained through the courtesy of A. C. Lilly at Philip Morris Research Laboratory.

Effects of γ-irradiation. - Mobility measurements were made both before and after a period of irradiation with Co-60 γ-rays. The irradiation

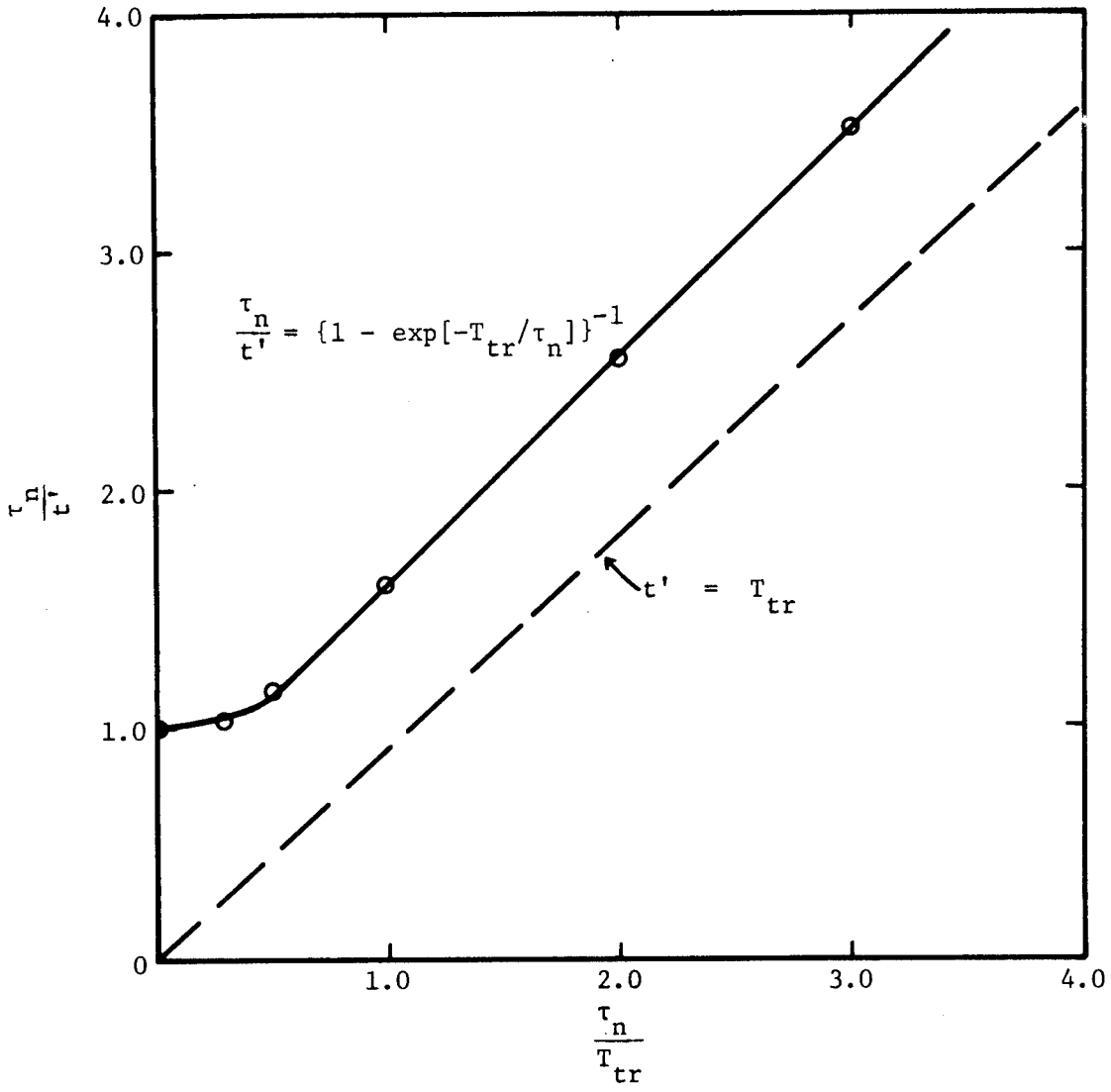

Figure 27. PLOT OF THE RELATION BETWEEN EFFECTIVE DRIFT TIME, t', AND THE CARRIER TRANSIT TIME, T_{tr}, NORMALIZED TO THE CARRIER LIFETIME, τ_n.

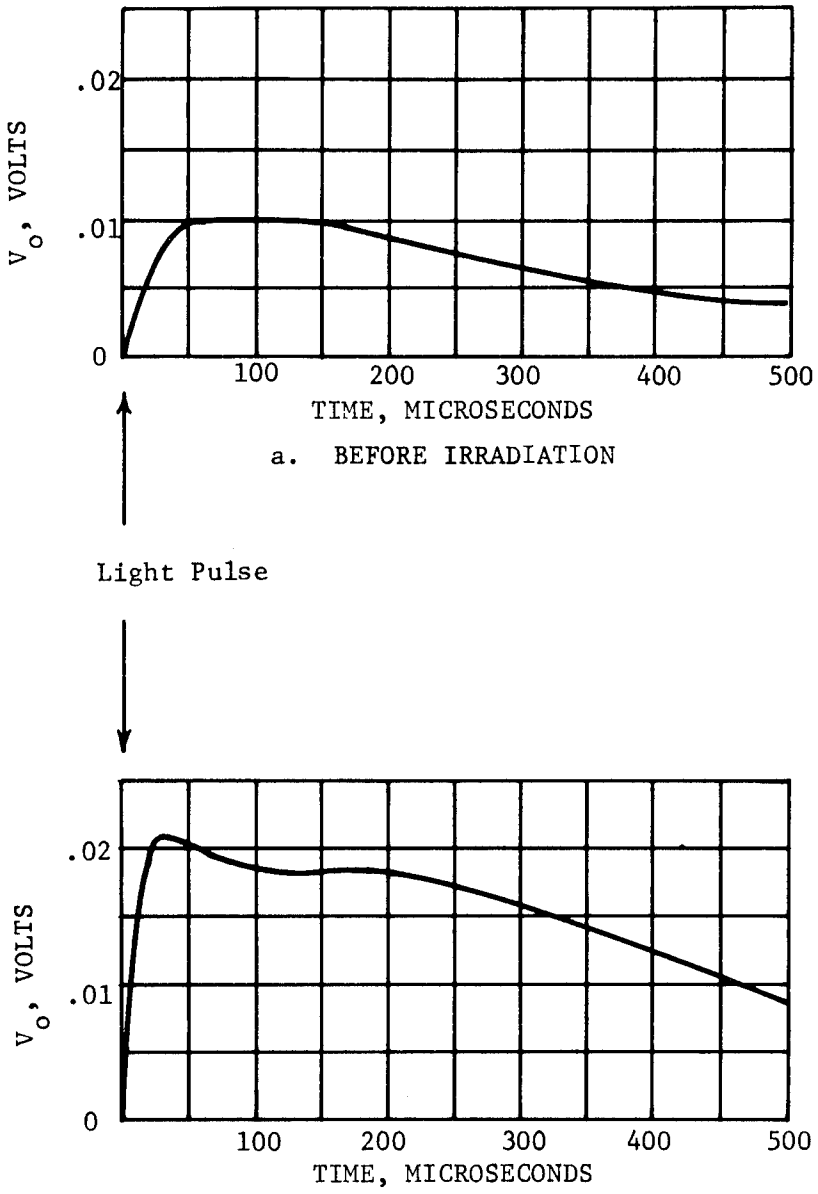

Figure 28. TIME OF FLIGHT PHOTORESPONSE ALONG THE A-AXIS OF DIMETHYLTEREPHTHALATE. Applied voltage = 200 volts, R = 10^5 ohms.

TABLE I

MEASURED CARRIER MOBILITIES IN MOLECULAR CRYSTALS

Crystal	Axis	Electron Mobility	Hole Mobility
Dimethylterephthalate	a	5 $cm^2V^{-1}sec^{-1}$	0.8 $cm^2V^{-1}sec^{-1}$
	101		0.8
	c		3
	⊥ to 101	15 - 70	10
Dibenzoate Ester of Ethylene Glycol	c		2
	a		0.7
Mylar Chip		0.2	
Mylar Film			2×10^{-3}

S-6128

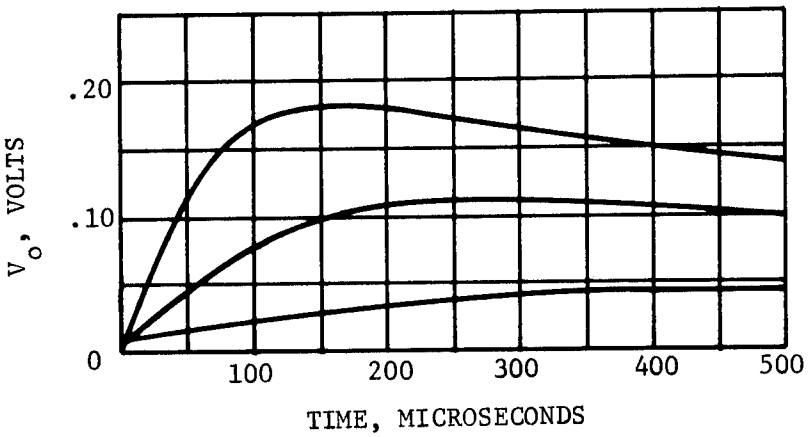

Figure 29. INTEGRATED TRANSIT TIME PULSE WITH TRAPPING FOR DIMETHYLTEREPHTHALATE. Applied voltage = 125, 400, 800 volts, R = 10^7 ohms, 5 days after irradiation of 12.4 Mrad.

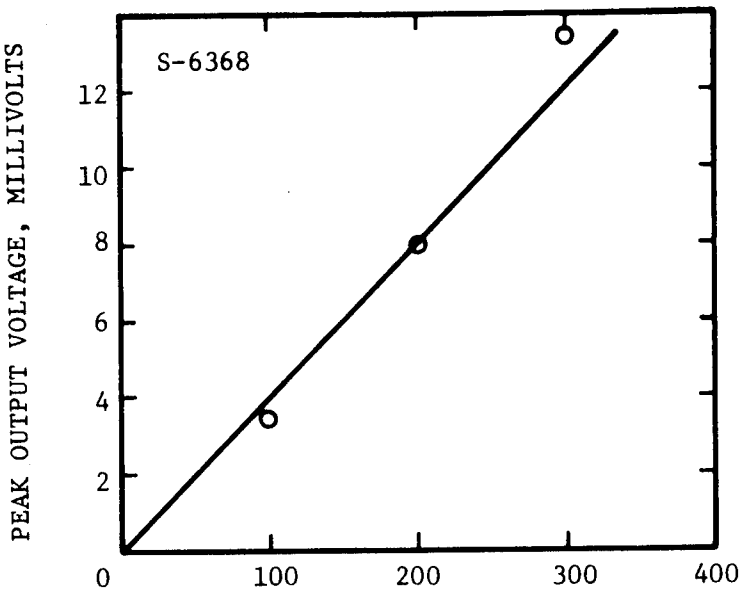

(a) PEAK OUTPUT VOLTAGE VERSUS APPLIED VOLTAGE

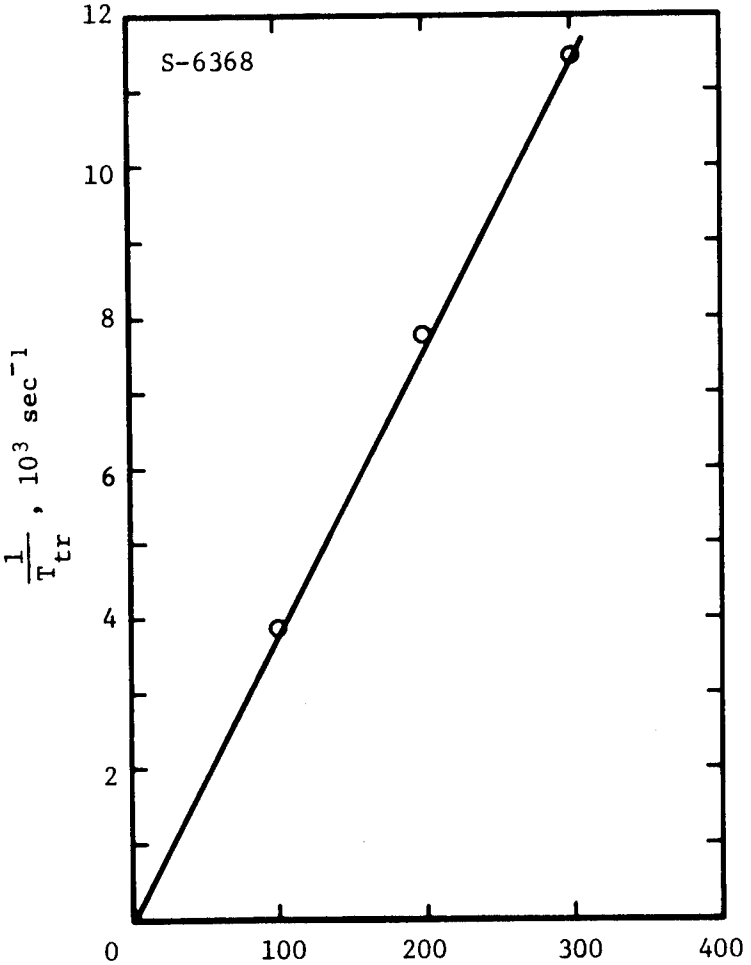

(b) INVERSE TRANSIT TIME VERSUS APPLIED VOLTAGE

Figure 30. TIME OF FLIGHT MEASUREMENTS PARALLEL TO THE 101-AXIS OF DIMETHYLTEREPHTHALATE. Tin oxide electrodes and xenon lamp, $A = .675^2$cm, L = 0.1 cm, $R = 10^5$ ohms.

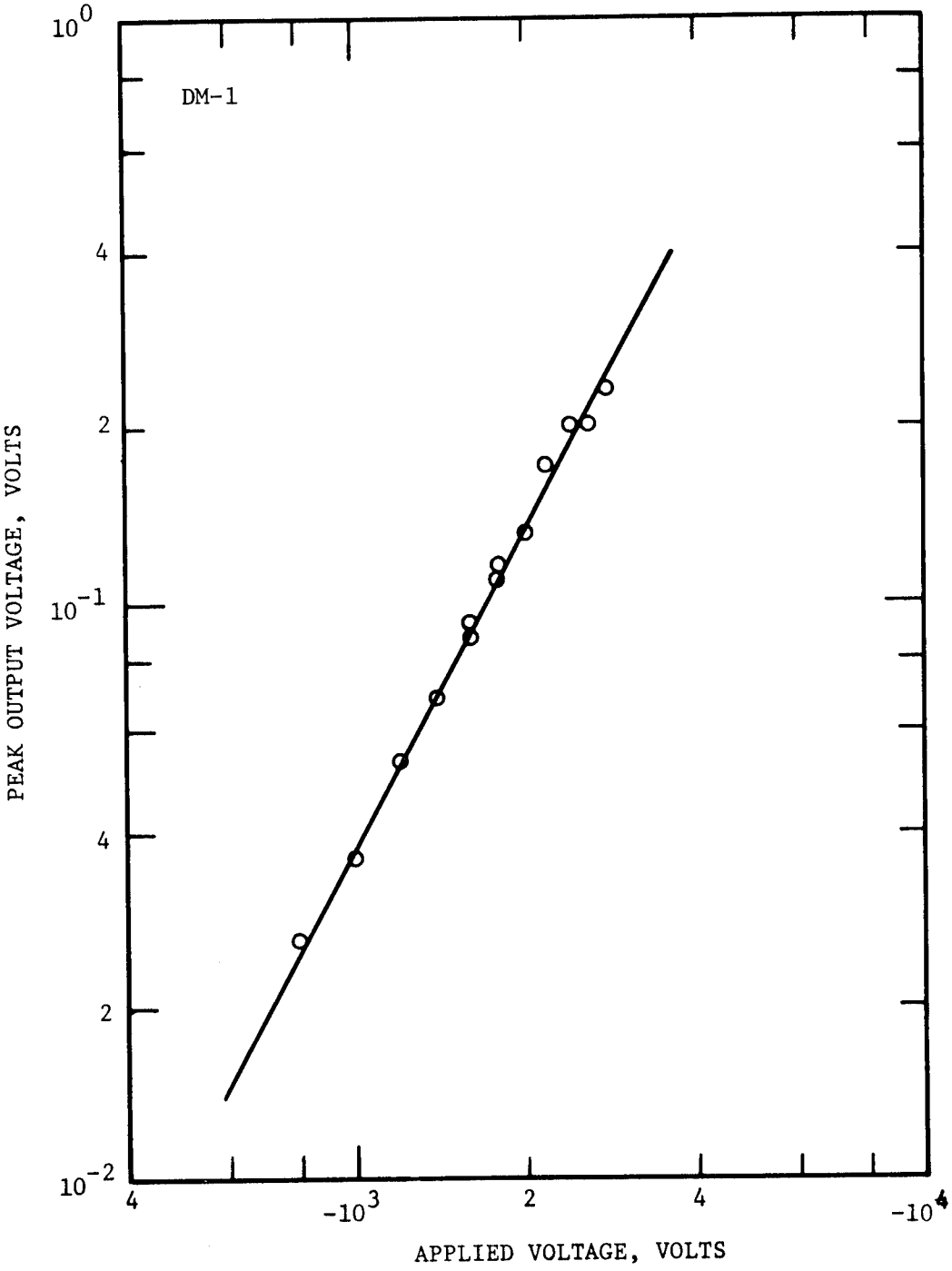

Figure 31. PEAK OUTPUT VOLTAGE VERSUS APPLIED VOLTAGE FOR A-AXIS OF DIMETHYLTEREPHTHALATE.
300 Å silver electrodes with silver paste guard ring, thickness = 0.45 cm, area = 0.37 cm^2, R = 7 x 10^5 ohms.

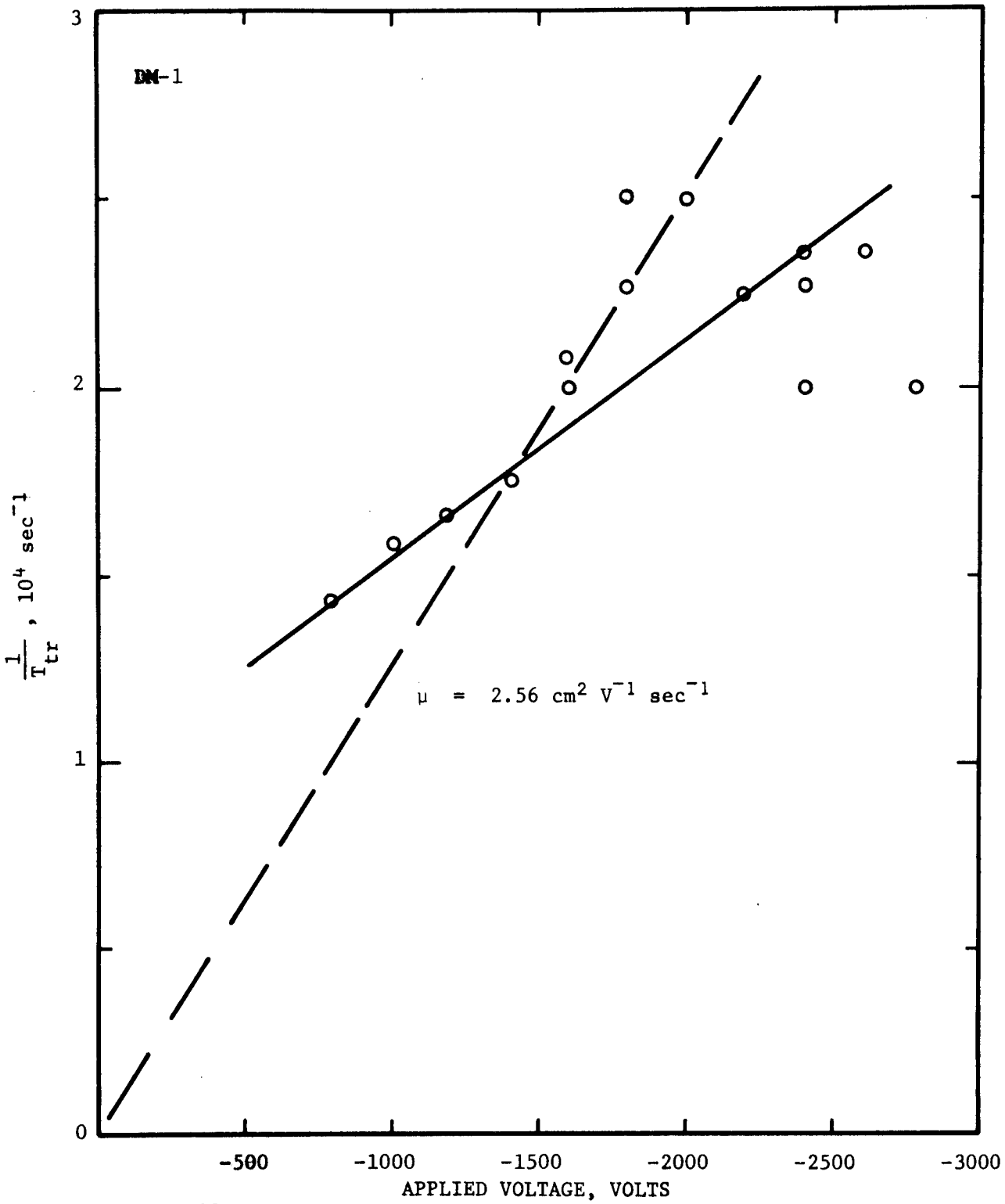

Figure 32. INVERSE TRANSIT TIME VERSUS APPLIED VOLTAGE FOR A-AXIS OF DIMETHYLTEREPHTHALATE.
300 A silver electrodes with silver paste guard ring, thickness = 0.45 cm, area = 0.37 cm^2, R = 7 x 10^5 ohms.

consisted of shorting the terminals of the sample holder of Fig. 10 and placing it in the irradiation facility. Measurements were made at various times after removal from the facility and a decrease in mobility was observed which continued to decrease with time even though no additional irradiation was received. Changes in the mobility as a function of dose received are shown in Fig. 33. For the sample designated S-6128 along the a-axis, the three points at 12.4 Mrads show the successive decrease in mobility with a time lapse of several weeks between measurements. Variation of the peak output voltage with applied voltage for this sample are shown in Fig. 34 using the pulse integrating circuitry. The decreasing slope of the curve at 800 volts may indicate that most of the charge generated is being collected at this point. A plot of the reciprocal effective drift time versus applied voltage is shown in Fig. 35 and Fig. 36. The time interval between the two measurements is approximately 2 weeks. As indicated in Fig. 27, extrapolation of the curve based on points where t^1 is small compared to τ_n should intersect the $\frac{1}{t^1}$ axis at $\frac{0.6}{T_n}$ as a rough approximation. This results in an estimate of 600 μsec for the hole lifetime for both cases. The slope and thus the mobility is lower, however, at the later time. The electrical conductivity of this sample was 5×10^{-15} $ohm^{-1}cm^{-1}$.

3.3.3 Mobility of Dibenzoate Ester of Ethylene Glycol (DEG)

The hole mobility along the c-axis of DEG was measured using the X-ray technique. The applied voltage required before the typical transit time peak was observed limited the number of experimental observations but definite motion of the peak with voltage was observed as well as an indication of fairly strong polarization of the internal field. At 3500 volts the transit time increased from 145 μsec to 185 μsec in 22 minutes. The sample dimensions were 0.9(L) x 0.2 x 0.06 cm^3. The mobility of 2 $cm^2\ V^{-1}\ sec^{-1}$ in Table I may be low as a consequence of uncertainty in the internal field.

The results of measurements along the a-axis are shown in Fig. 37 using tin oxide electrodes. The peak photocurrent varies somewhat less than quadratically with voltage. Although the plot of inverse transit time versus applied voltage is inconclusive, there is probably a small trapping effect. Polarization effects were either stable, on the order of minutes, or not present along this axis.

The mobility before irradiation was 0.7 $cm^2\ V^{-1}\ sec^{-1}$. After a dose of 8.6 Mrads this was reduced to 0.65 $cm^2\ V^{-1}\ sec^{-1}$.

3.3.4 Mobility of Poly(ethylene terephthalate)

In general, the data from time of flight measurements on PET cannot be interpreted in terms of charge carrier mobility. The dominant

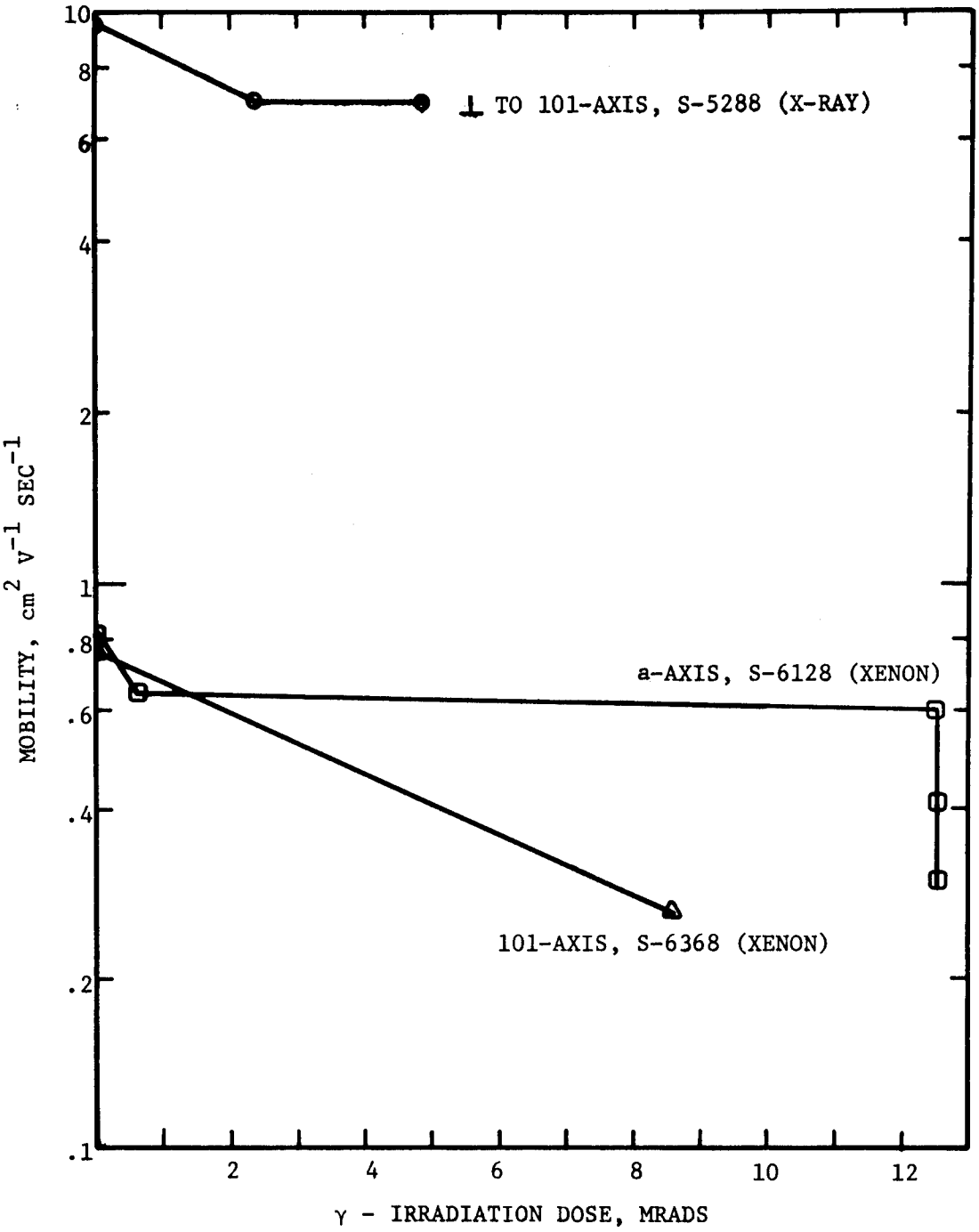

Figure 33. EFFECT OF γ - IRRADIATION ON HOLE MOBILITY IN DIMETHYLTEREPHTHALATE.

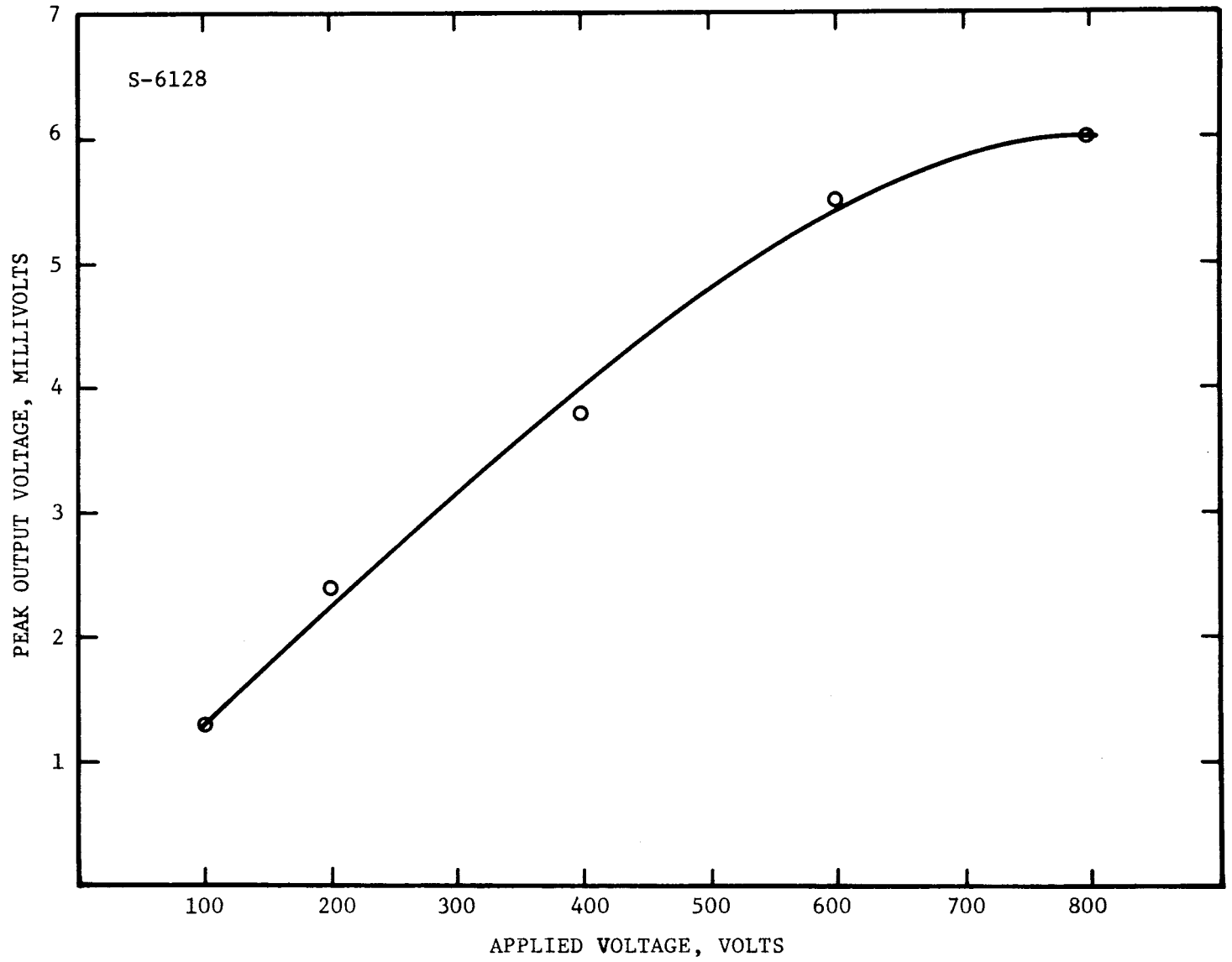

Figure 34. VARIATION OF PEAK PHOTORESPONSE WITH APPLIED VOLTAGE FOR THE A-AXIS OF DIMETHYLTEREPHTHALATE

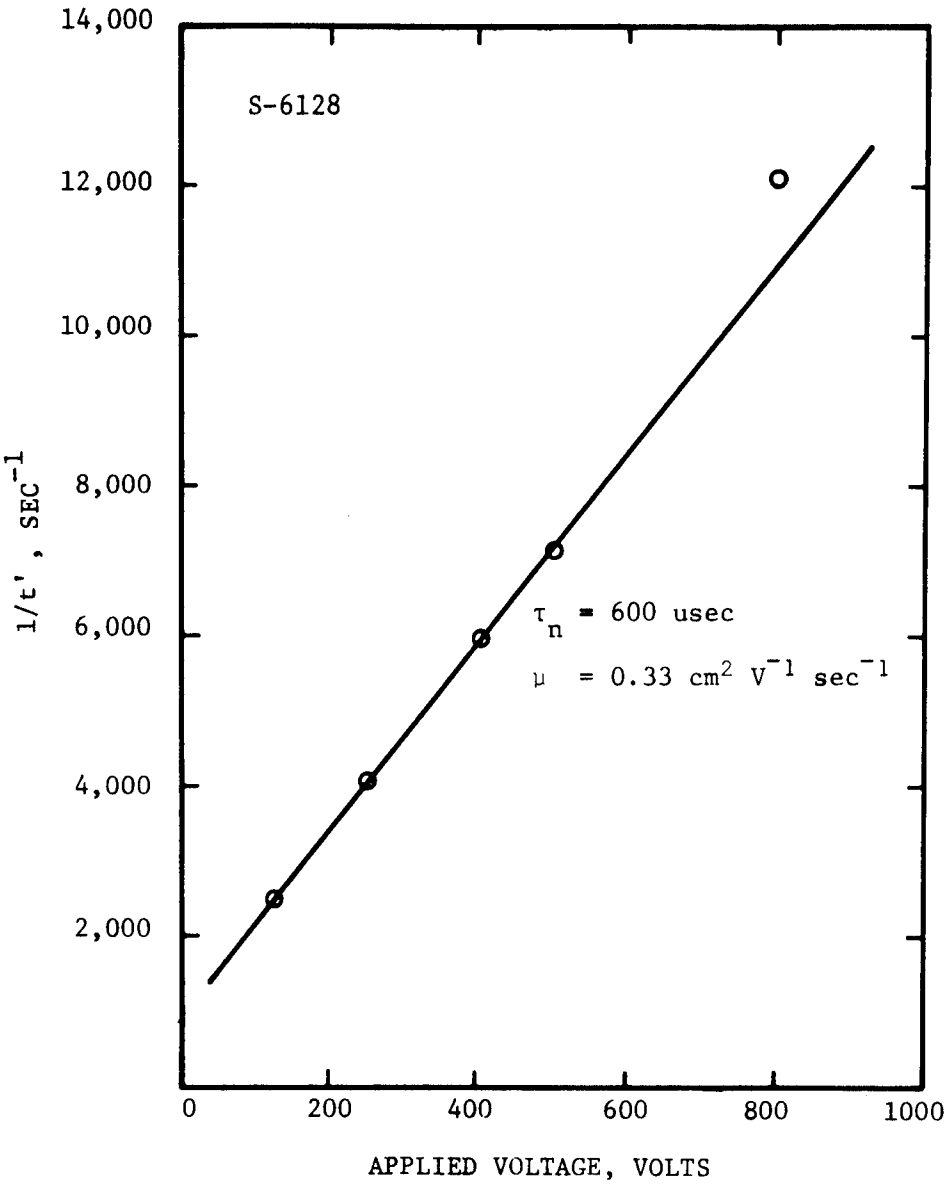

Figure 35. RECIPROCAL EFFECTIVE DRIFT TIME VERSUS APPLIED VOLTAGE ALONG THE A-AXIS OF DIMETHYLTEREPHTHALATE. Measurement taken 5 days after γ-irradiation of 12.4 Mrad.

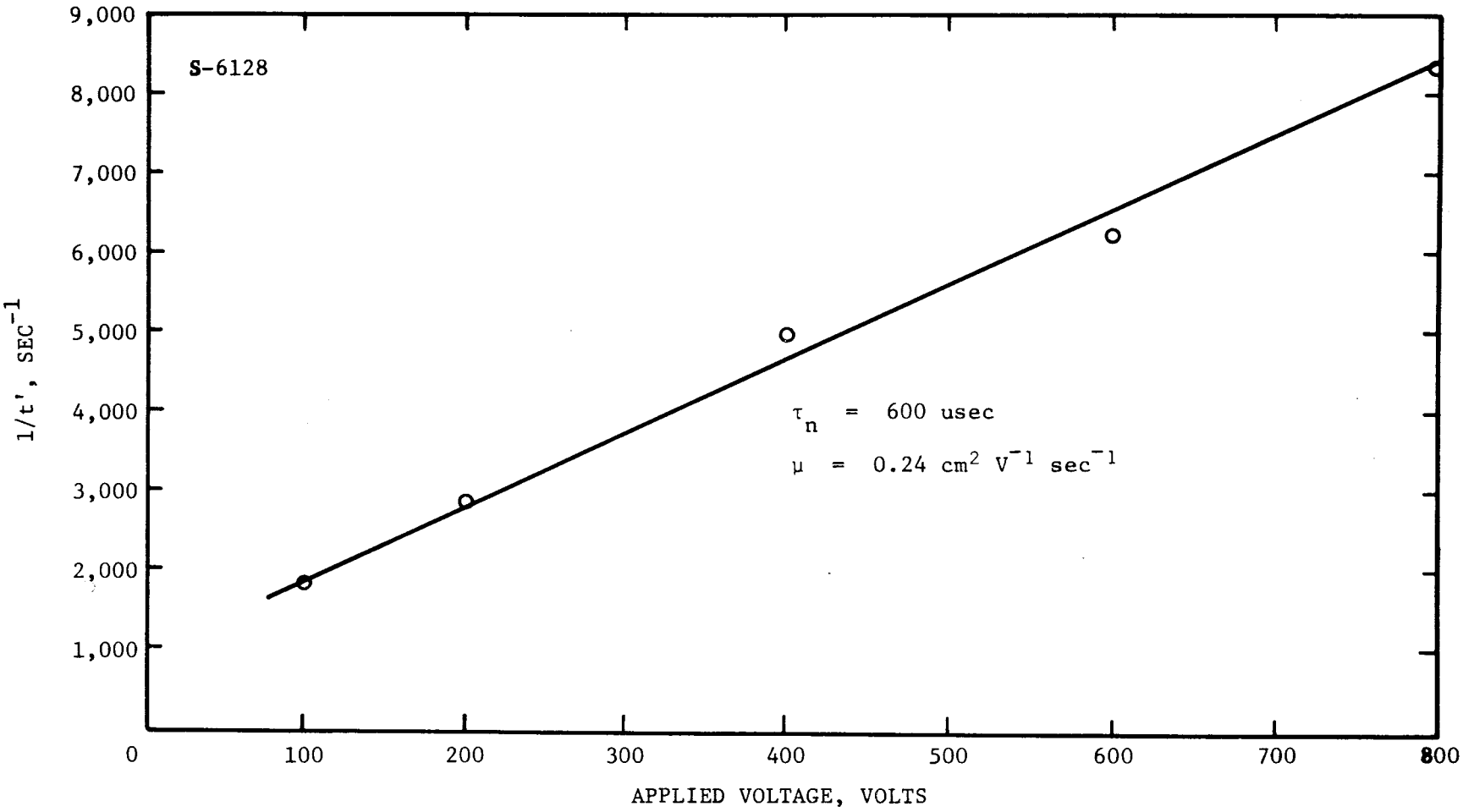

Figure 36. RECIPROCAL EFFECTIVE DRIFT TIME VERSUS APPLIED VOLTAGE ALONG THE A-AXIS OF DIMETHYLTEREPHTHALATE Measurement taken 17 days after γ-irradiation of 12.4 Mrads.

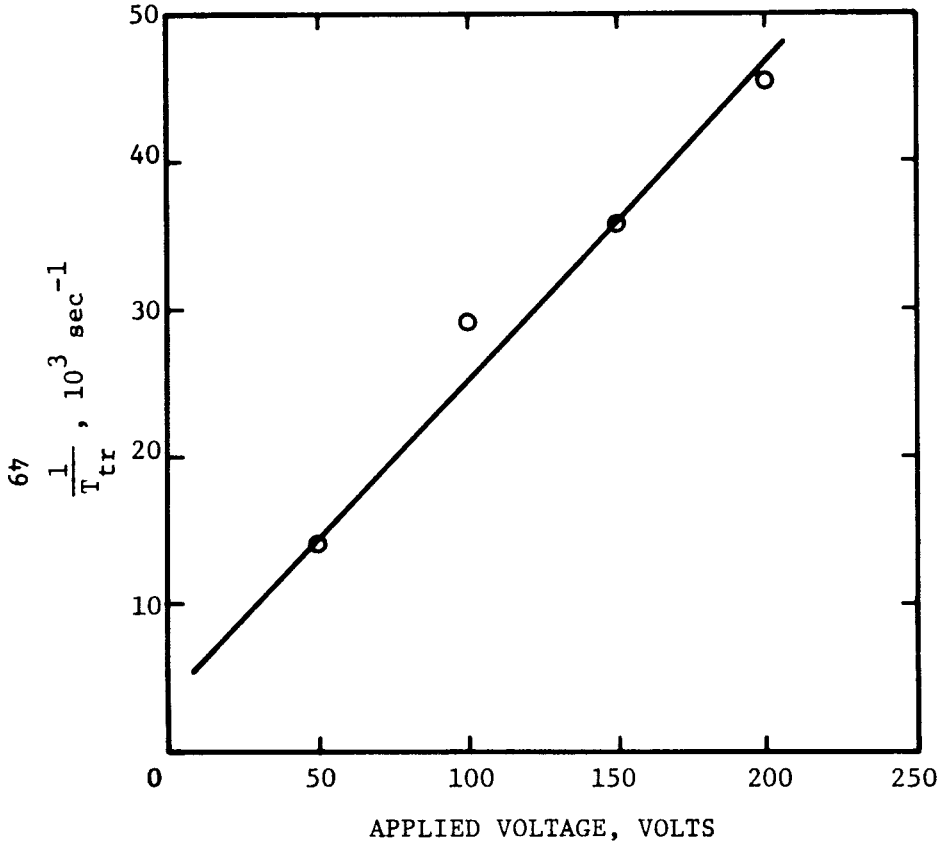

(a) INVERSE TRANSIT TIME VERSUS APPLIED VOLTAGE

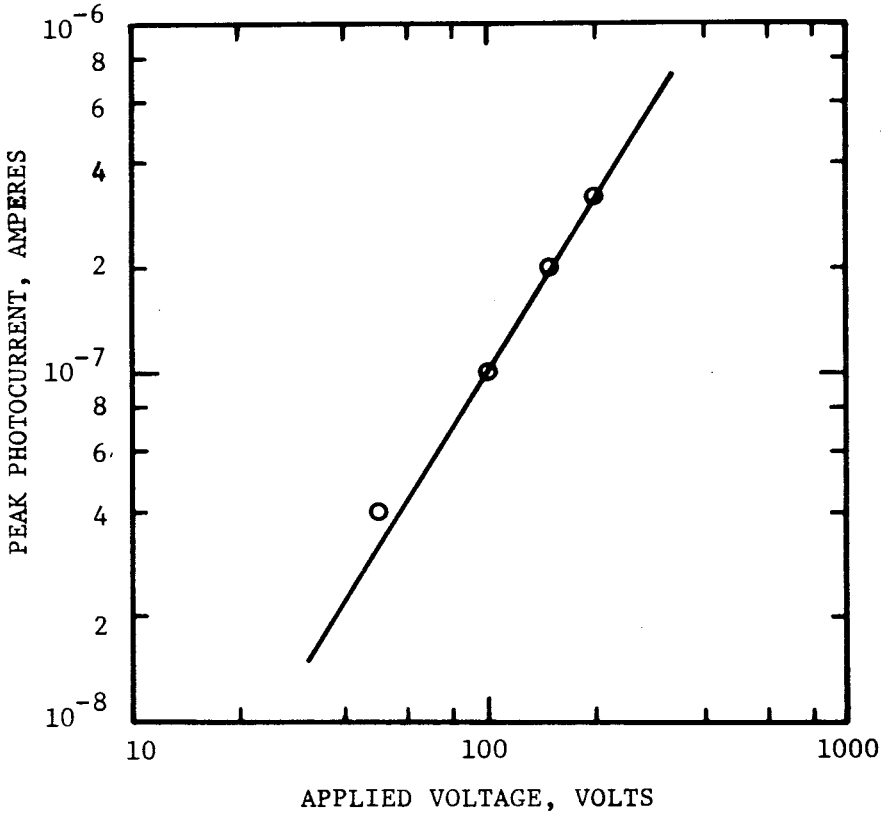

(b) PEAK PHOTOCURRENT VERSUS APPLIED VOLTAGE

Figure 37. TIME OF FLIGHT MEASUREMENTS ALONG THE A-AXIS OF DIBENZOATE ESTHER OF ETHYLENE GLYCOL. Tin oxide electrodes, A = 0.15 cm^2, L = 0.05 cm, R = 10^5 ohms.

features of photoresponse appear to be trapping and polarization at the electrode surface and in the bulk. On one occasion, however, measurements were performed using a solution of salt (NaCl) and water for the electrodes which appeared to give a trap-free response. These data are plotted in Fig. 38. The solid line corresponds to a hole mobility of 2.2×10^{-3} cm^2 V^{-1} sec^{-1}. In Fig. 39 the results of an integrating technique are shown. These results indicate a very short carrier lifetime which dictates that time of flight measurements would not yield a dependable value for the mobility. Although the sensitivity of the integrating technique in Fig. 38 is very low, the solid curve can be used to obtain an estimate of the mobility in PET. Based on these data, one would arrive at a carrier lifetime of about 10 microseconds and a mobility of 2×10^{-3} cm^2 V^{-1} sec^{-1}. The agreement between this value and the time of flight result above is fortuitous since it is better than one expected considering the experimental errors involved.

In order to shed some additional light upon the PET system, some observations were made using Mylar chips. When these chips were irradiated with the X-ray pulse, a characteristic peak was observed which shifted with voltage in the time of flight manner. The electrode area composed of silver paint was 0.32 cm^2. The thickness (L) was 0.2 cm. Using the data at 3500 Volts, the electron mobility was calculated to be .21 $cm^2V^{-1}sec^{-1}$. Additional study is necessary in order to correlate these results with the drawn PET film samples.

3.4 Polarization and Photoresponse

Early in the experimental program it was evident that sample polarization is very complicated in PET. In order to characterize this polarization in terms of time, photon irradiation, and spatial distribution, several samples of different thicknesses were prepared with 300 Å silver electrodes. The peak photocurrent resulting from a Hg-arc flash lamp was recorded as I_{PO}. The sample was then exposed continuously in a high intensity Hg-arc lamp for various irradiation times up to 150 minutes. The sample is then irradiated a second time with the Hg-arc flash and the peak photocurrent recorded as I_P. The difference between I_{PO} and I_P is shown in Fig. 40.

A rather surprising photoresponse was observed in PET under the conditions of sample A-7118. With a negative voltage of 100 volts applied to the front electrode the pulse observed was a positive pulse of large magnitude. The sample was exposed under a vacuum with 830 Å of aluminum on the back electrode and 300 Å of silver on the front electrode. The peak in the initial portion of the pulse was independent of the input impedance or the pulse shape as is shown in Fig. 41 for an input impedance of 10^5 ohms and an impedance of 10^7 ohms. This pulse is described as a depolarization photo pulse because of its characteristics with respect to the amount of time the voltage was applied to the sample before the photon flash occurred. A plot of the magnitude of the output voltage

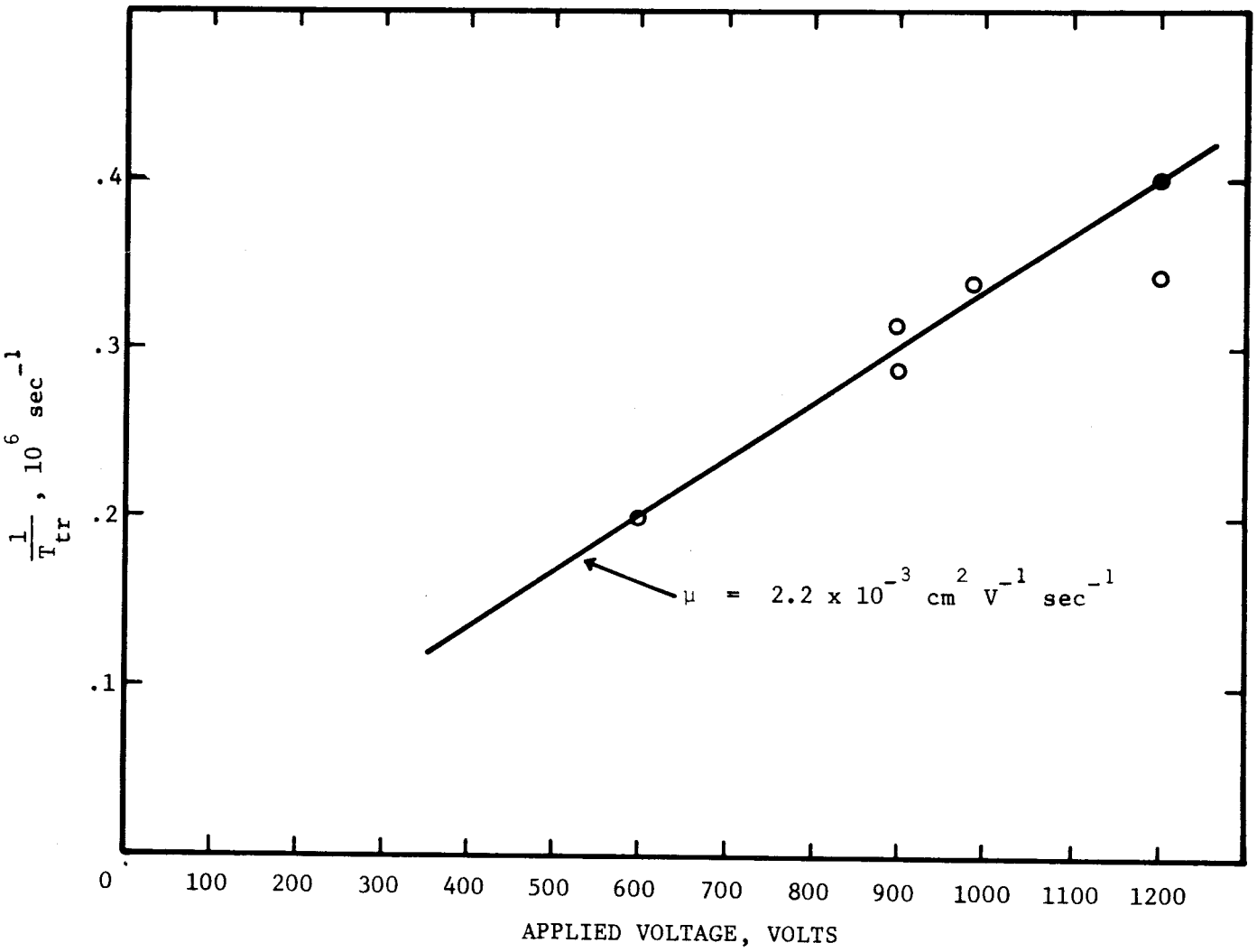

FIGURE 38. INVERSE TRANSIT TIME VERSUS VOLTAGE FOR 1 MIL PET
Mercury Lamp, Sodium Chloride Electrodes

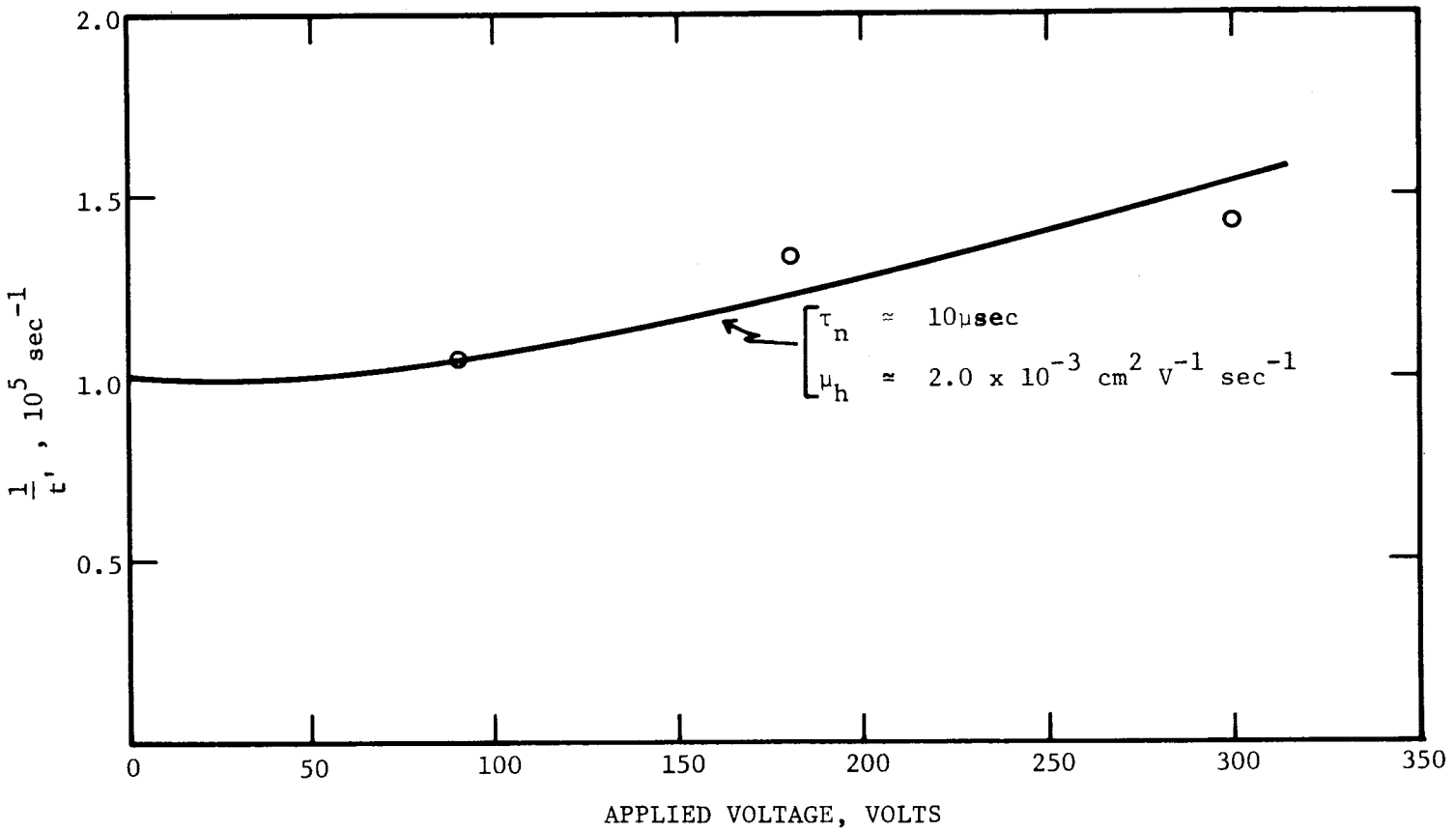

FIGURE 39. INVERSE EFFECTIVE DRIFT TIME VERSUS VOLTAGE FOR 1 MIL PET

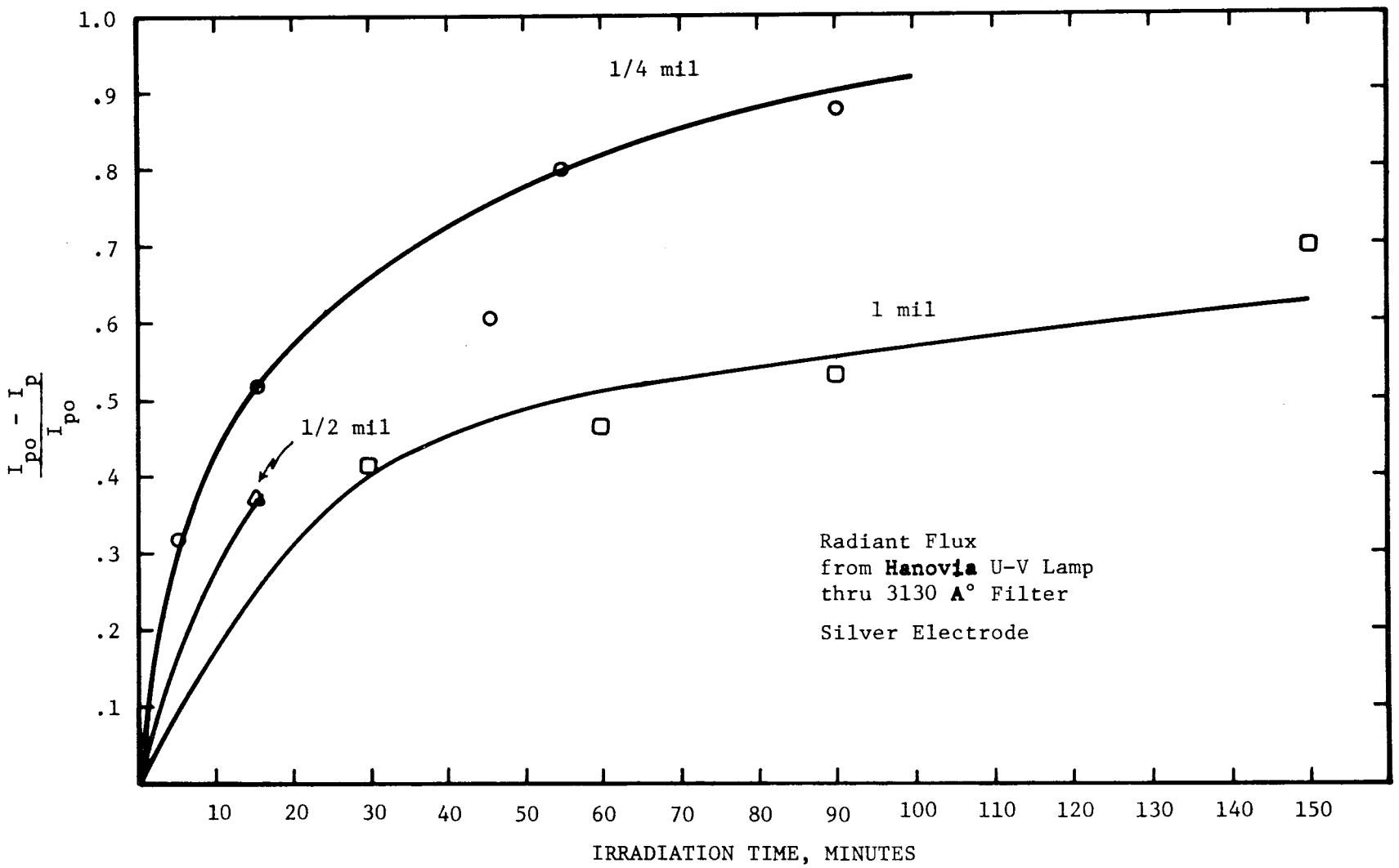

FIGURE 40. ATTENUATION OF PHOTOCURRENT PEAK BY EXPOSURE TO U-V LIGHT

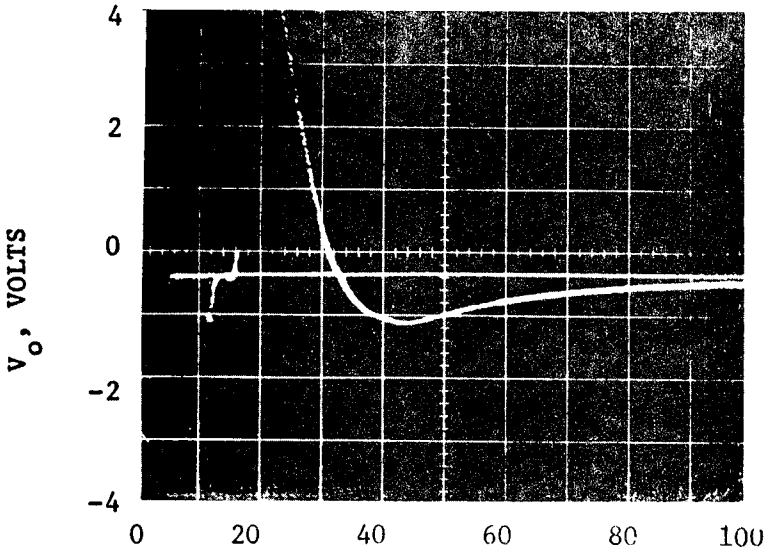

a. OUTPUT VOLTAGE PULSE ACROSS 10^5 OHMS.

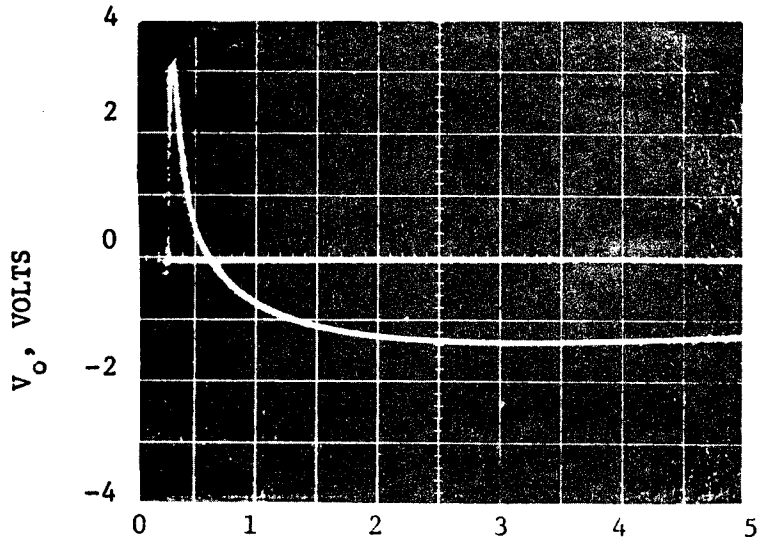

b. OUTPUT VOLTAGE PULSE ACROSS 10^7 OHMS

Figure 41. PHOTORESPONSE OF 1 MIL PET TO XENON FLASH LAMP. Applied voltage = -100 volts to front electrode, 300A° silver on front electrode, 830A° Aluminum on back electrode, area = 3.88 cm^2.

as a function of the delay time after voltage is applied is shown in Fig. 42. For a very short delay time the sample has had little time to polarize and the observed output pulse is very small. As the polarization time increases, the photo pulse observed becomes very large. The region of the sample in which this effect occurs was demonstrated to be less than 1/4 mil. By placing a 1/4 mil PET sample between the light and the sample upon which the voltage is applied, the photoresponse was reduced to a negligible value. These experiments show clearly the influence of electrode material and environmental history on the polarization and photoresponse of PET.

3.5 Charge Storage and Breakdown in Irradiated Inorganic Films

Three types of dielectrics in capacitor type structures were fabricated and irradiated during this experiment. The MOS structures tested were (1) silicon dioxide, (2) silicon monoxide, and (3) aluminum oxide. The dielectrics were deposited or grown on n and p type silicon substrates with a thin aluminum electrode approximately 1000 Å thick through which the electron flux penetrated. The first MOS structure was prepared using silicon dioxide (SiO_2) thermally grown with steam in an oxidation furnace. These samples had oxide thicknesses of 5000 and 15,000 Å. The second type structure was prepared by vacuum deposition of silicon monoxide (SiO) while maintaining a substrate temperature in excess of 150°C. After cooling the samples were removed and placed in an oxidation furnace for 5 minutes in an oxygen environment. Oxide thicknesses for SiO structures were 5000 Å and 15,000 Å. The third capacitor used aluminum oxide (Al_2O_3) for the dielectric which was pyrolytically deposited with a substrate temperature of 640°C. The deposition required approximately 15 minutes for an oxide thickness of 2500 Å. After depositing the dielectric on the silicon substrates, the samples were placed in a vacuum system for evaporating aluminum to approximately 1000 Å thick for the top electrode.

Measurement of charge storage and detection of spontaneous discharges were performed on capacitors with dielectrics of SiO_2, SiO, and Al_2O_3 using monoenergetic electrons. Electron flux densities used in the irradiations were 10^9, 10^{10}, 10^{11}, and 10^{12} e/cm^2 sec. During the investigation the capacitors were tested at -142°C, 27°C, and 90°C. For charge storage measurement the irradiations were conducted at fluences in the range between 10^{10} and 10^{14} e/cm^2. Charge storage measurements utilized either capacitance versus voltage (C-V) or external charge transfer technique.

Fluences ranged between 10^{12} and 10^{16} e/cm^2 for the spontaneous discharge experiment. The lower values of fluence correspond to the very low electron flux densities. Electron energies used for the spontaneous discharge experiment had a range corresponding to a one-half thickness for each dielectric. The measurement circuit was

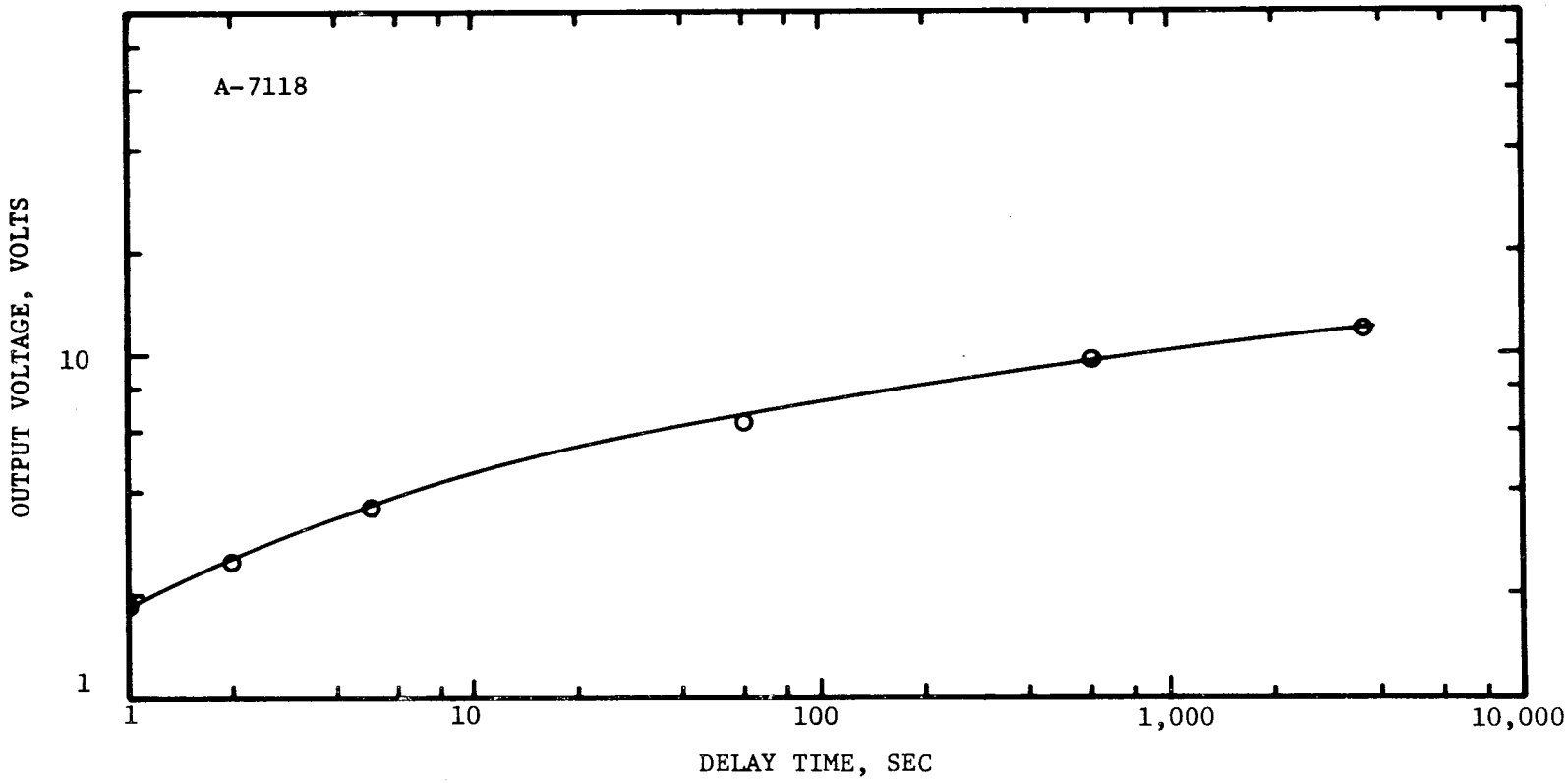

Figure 42. PEAK PHOTORESPONSE OF 1 MIL PET VERSUS DELAY TIME BETWEEN VOLTAGE APPLICATION AND PHOTON PULSE. Applied voltage = -100 volts, 830 Å of aluminum on back electrode, 300 Å of aluminum on front electrode, sample under vacuum

capable of detecting 10 mV pulses, however, as a result of noise in the irradiation facility due to beam current fluctuations, and extraneous sources, the discrimination level was approximately 30 millivolts for the measuring circuit. The sample was connected to the input of an electrometer. The input impedance of the electrometer and the capacitance of the irradiated sample determined the decay time constant of the discharge pulse. A strip chart was connected to the electrometer output to monitor the samples. This provides a discrimination technique whereby only those pulses with the proper decay time constant are counted.

In the spontaneous discharge experiment the capacitors with SiO and SiO_2 dielectrics were irradiated with 5 and 10 KeV electrons at three temperatures. The structures were exposed to fluence levels in excess of 10^{14} e/cm^2 except the irradiations performed using electron flux densities less than 10^{10} e/cm^2 sec. Typical values of capacitance for SiO_2 0.5 and 1.5μ thick were 8.8 and 2.2 nanofarads respectively. For the samples of SiO dielectric thickness of 0.5 and 1.5μ had typical values of capacitance of 15.1 and 6.2 nanofarads. Due to difficulty in obtaining satisfactory large area samples of Al_2O_3 the electrode area was reduced. Capacitor structures using Al_2O_3 dielectrics had a typical capacitance value of 0.2 nanofarads. Al_2O_3 samples were irradiated with 5 KeV electrons and received a fluence greater than 10^{14} e/cm^2. Approximately ten samples of SiO, SiO_2, and Al_2O_3 were irradiated in attempts to induce spontaneous discharges. No spontaneous discharges were detected in excess of the discrimination level of 30 millivolts.

Samples of SiO_2, SiO, and Al_2O_3, were irradiated at 5 and 10 Kev with electron flux densities 10^9, 10^{10}, 10^{11}, and 10^{12} e/cm^2 sec which yielded a fluence ranging between 10^{12} and 6×10^{14} e/cm^2. The samples were shorted during the irradiation period and 30 seconds after the exposure. The samples then were immediately connected to an electrometer to observe the external current in the circuit. No measurable current was observed in the external circuit for sample with dielectrics of SiO_2 and Al_2O_3. Samples with evaporated SiO for the dielectric were irradiated and current was observed as shown in Fig. 43.

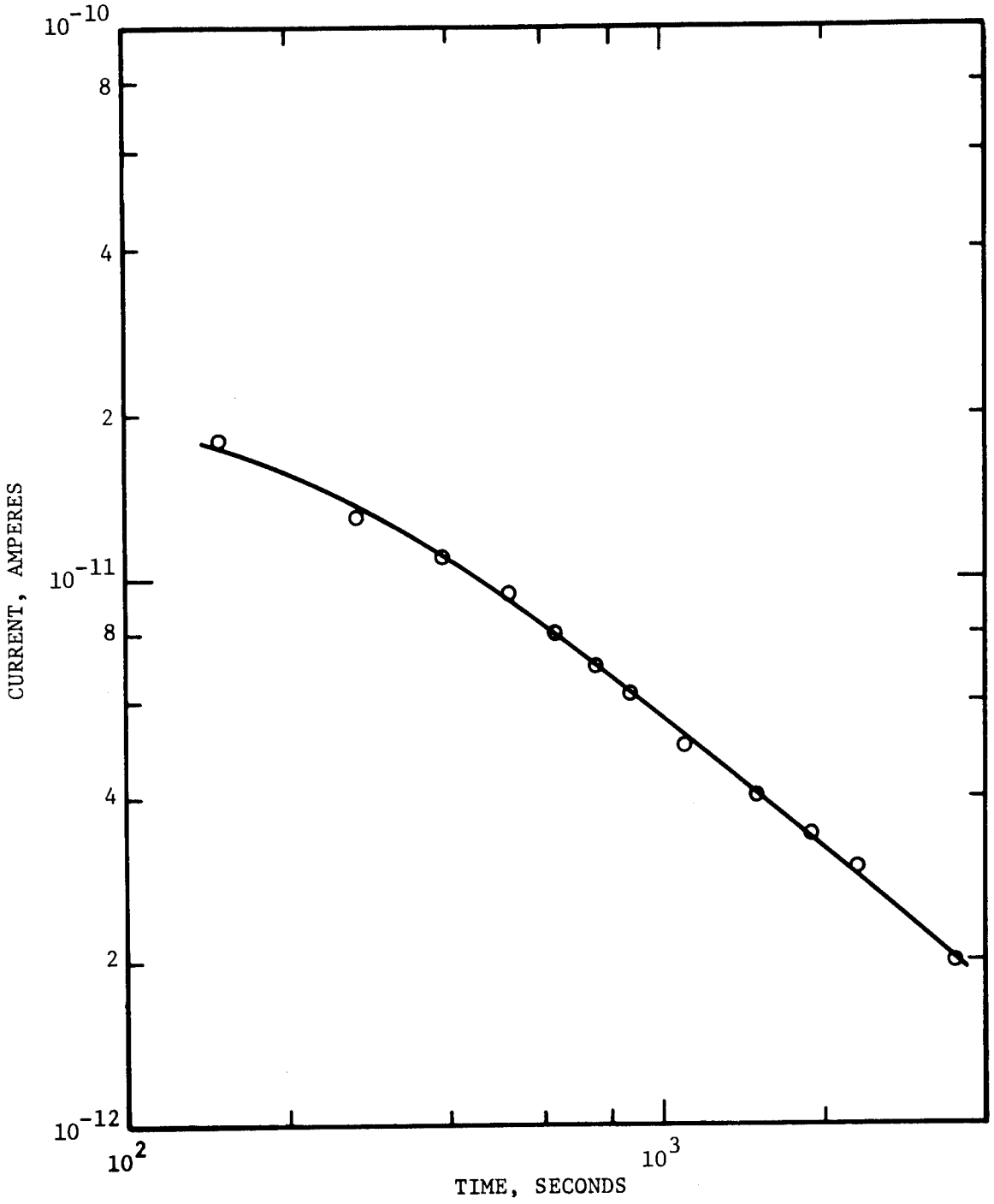

Figure 43. SHORT CIRCUIT CURRENT IN 5000Å FILM OF SiO AFTER ELECTRON IRRADIATION.
Electron energy = 5 KW, beam current = 5×10^{-8} amps/cm^2, irradiation time = 240 sec.

SECTION IV

SUMMARY AND CONCLUSIONS

The formation of free radicals in PET can be initiated by exposure to γ-rays or UV light. As the concentration of radicals increases, there is a simultaneous increase in the electrical conductivity as well as the optical absorption coefficient near 3100A°.

Based on the analysis of ESR signals, three distinct radicals are observed. It is postulated that these radicals (I, II, and III) are directly responsible for the electrical and optical changes which were observed in PET. The parallel behavior of the decay kinetics of radical II concentration and the conductivity under certain conditions substantiated this relationship. The quenching effects of oxygen are also in agreement. Since different types of PET samples behave differently each type must be analyzed separately according to its degree of crystallinity.

Amorphous PET. - The amorphous samples are believed to contain radical II and III. Upon heating the radicals decay and the relative proportion of radical III increases. After an initially rapid reaction the decay of the radical population conforms to second order kinetics. An Arrhenius plot of the logarithm of specific rate versus the reciprocal absdute temperature results in two lines which intersect at 72°C. This is very close to the glass transition temperature, T_g = 70°C. The activation energies are 112 Kcal/mole above 72°C, and 25 Kcal/mole below 72°C. Reference to reports in the literature suggest that this decay can be explained by long range movement of the polymer molecules, even in the glassy solid.

The buildup of conductivity in amorphous PET occurs as the radical concentration increases. (Not in a directly proportional manner at low γ-dose levels.) The decrease in conductivity after termination of γ-irradiation conforms to second order kinetics as does the radical decay. An Arrhenius plot of the specific rate yields an activation energy of 101 Kcal/mole which compares well with the results for radical decay. The conductivity in amorphous samples is due primarily to radical II.

Biaxially-oriented PET. - The crystallinity of these samples is about 50%. The decay of radical I in the crystalline regions of an oriented sample follows first order kinetics. As the decay occurs at temperatures as low as 110°C (The melting point is about 255°C) it seems that decay by normal physical movement is unlikely. Chemical

migration of free radical sites by hydrogen atom hopping is a more reasonable explanation.

Radical buildup in biaxially oriented PET as observed from ESR spectra follows very closely the conductivity buildup observed in a similar sample under gamma irradiation. The decay of conductivity conforms to first order kinetics. The specific rate constant is not in agreement with the results for radical decay although comparison under identical conditions has not been achieved.

Crystalline PET. - Samples of about 70% crystallinity exhibit a total γ-induced radical concentration about the same as amorphous samples but composed primarily of radicals I and III. Radical decay kinetics in this case are not simple. Radical III which was found to be present in both the amorphous as well as partially crystalline samples was not correlated to any specific electrical properties; however, since its presence indicates a certain chemical memory, some of the irregularities which are often observed in electrical properties of PET could well be associated with the previous history of the sample and the concentration of radical III.

Oxygen Quenching. - The presence of oxygen rapidly decreases the radiation induced radical concentration in PET. That these radicals are the basis of electrical conductivity and optical absorbance is supported by the concurrent behavior of these two phenomena. Oxygen causes the absorption spectra near 3100 Å to decrease although it never returns to its previous value before irradiation.

The electrical conductivity of an irradiated sample is drastically reduced upon access to oxygen. Greater than 3 orders of magnitude reduction in conductivity is observed after exposure for about one minute.

Electronic Measurements. - Polarization was a dominant parameter in the interpretation of the electronic measurements. This was true in particular as a variety of contacts was applied to PET film. Particular aspects of polarization which were observed included (1) a reduction of polarization in a gamma field, (2) a photoresponse comparable in effect to photo-depolarization, (3) reduction of photo-sensitivity by previous radiation history, (4) a reduction of observed mobility in molecular crystals, and (5) variation of observed photo-response as a function of electrode material. The electron mobility of PET was measured using two different techniques, one a time-of-flight measurement and the other an integrating technique. Both techniques resulted in a value of 2×10^{-3} cm^2 $V^{-1}sec^{-1}$. At the present time this value carries a low degree of confidence due to the many occasions in which no usable data could be obtained. In this case, usable refers to the proper variance with voltage of the transit time and the photo-peak. Both electron and hole mobilities were observed in the molecular crystals of the dibenzoate of ethyleneglycol and dimethylterephthalate.

The mobilities ranged from 10 to .2 cm^2/Vsec depending upon the crystal orientation. One of the primary purposes for measuring the mobility is the usefulness of this parameter in specifying electrical conductivity and in the possibility of measuring this parameter before and after a period of gamma irradiation. It was found that gamma irradiation resulted in a large reduction in the observed mobility. Reductions were on the order of 25 to 50% for doses of around 10 Mrads. The full effect of radiation was sometimes delayed several weeks after the period of radiation. The results were obtained in an air environment. Indications of large changes which depend on the environment were observed.

Attempts to measure charge release currents in other dielectrics included silicon dioxide, silicon monoxide, and Al_2O_3. Under fluences ranging between 10^{12} and 10^{14} e/cm^2, only the silicon monoxide exhibited any observable current.

REFERENCES

1a. S. Ohnishi, S. Sugimoto, and I. Nitta, J. Chem. Phys., 39, 2647 (1963).

1b. S. Ohnishi and I. Nitta, J. Polymer Sci., 38, 451 (1959).

2. D. S. Ballantine and Y. Schinohara, 5th International Symposium on Free Radicals, Session B3 (No. 5), Uppsala (1961).

3. M. Dole, C. D. Keeling, and D. G. Rose, J. Am. Chem. Soc., 76, 4304 (1954). See also M. Dole in "Crystalline Olefin Polymers" Part 1, Eds. R. A. V. Raff, and K. W. Doak, Intersciences Publishers (1965).

4. D. O. Yehmer and C. D. Wagner, Natose, 208, 72 (1965).

5. A. Charlesby, D. Libby, and M. G. Ormerod, Proc. Royal Soc., A262, 207 (1961).

6. I. Auerbach, Polymer 7, 283 (1966).

7. H. Sobue, Y. Tabata, and M. Hiraoka, Kogyo Kagaku Zasshi, 64, 372 (1961). Y. Hama, S. Okamoto, and N. Tamura, Reports on Progress in Polymer Phys., Japan, 7, 351 (1964).

8. D. Campbell and D. T. Turner, J. Polymer Sci., A-1, 5, 2199 (1967).

9. D. Campbell, K. Araki, and D. T. Turner, J. Polymer Sci., A-1, 4, 2597 (1966).

10. B. R. Loy, J. Polymer Sci., 44, 341 (1960)

11. H. J. Kolb and E. F. Izard, J. Appl. Phys. 20, 564 (1949).

12. F. Bueche, "Physical Properties of Polymers," Interscience (1962).

13. S. Shida, J. Higuchi, R. Kasaka, and T. Miyamae, cited in ref. 1.

14. G. S. Y. Yeh and P. H. Geil, J. Macromol. Sci. (Phys.), B1(2), 235 (1967).

15. D. Campbell and D. T. Turner, Polymer Letters, in press.

16. W. O. Statton, J. Polymer Sci., 41, 143 (1959).

17. J. C. Collier and E. Baer, Technical Report No. 20, Case Institute of Technology, (1966).

18. J. F. Fowler, Proc. Roy. Soc., London, A-236, 464 (1956).

19. V. L. Tal'rose and E. L. Frankevich, Dokl. Akad. Nauk SSR 129, 858 (1959).

20. M. A. Seitz, Ph.D. Dissertation, Northwestern University, 1966.

21. R. G. Kepler, Phys. Rev. 119, No. 4, 1226 (1960).